# Chapter 12
# Molecular and Structural Properties of Spider Silk

**Taylor Crawford, Caroline Williams, Ryan Hekman, Simmone Dyrness, Alisa Arata, and Craig Vierra**

**Abstract** Spider silk has extraordinary mechanical properties, outperforming some of the best-known man-made and natural materials in the world. Over the past 300 million years, spiders have evolved to produce high performance fibers that are uniquely designed to encompass high-tensile strength and toughness. As scientists have pursued a deeper understanding of the biochemical properties of silk, investigators have discovered that spiders are capable of spinning multiple fiber types that exhibit diverse mechanical properties. These differences are largely attributed to unique combinations of silk proteins spun into the fibers and the primary, secondary, and tertiary structure of the silk proteins in the fibers. Because of the outstanding properties of spider silk and its potential to serve as a next generation biomaterial, researchers have been racing to replicate synthetic spider silk. In this book chapter, we summarize the molecular and chemical properties of different silk types in spiders, their biological functions, and mechanisms of silk extrusion, assembly, and post-spin draw. We also discuss strategies that are being implemented for large-scale production of recombinant silk proteins using a variety of heterologous expression systems, explore purification protocols, and review the different spinning methodologies that are being applied for synthetic silk production.

## 12.1 Introduction

Over the past three decades, the number of reviews, books, and scientific research articles highlighting the material properties of spider silk has been increasing at a rapid rate. More than 45,000 species of spiders (class Arachnida, order Araneae) and a large number of aquatic and terrestrial insects, notably in the order Lepidoptera, have evolved the ability to spin silk. Silks are defined as fibrous material that is extruded into the environment, largely being comprised of proteinaceous

T. Crawford • C. Williams • R. Hekman • S. Dyrness • A. Arata • C. Vierra (✉)
Department of Biological Sciences, University of the Pacific, Stockton, CA 95211, USA
e-mail: taylor.rabara@gmail.com; cwilliams2@pacific.edu; rhekman@pacific.edu; simmonedyrness@gmail.com; aarata@u.pacific.edu; cvierra@pacific.edu



E. Cohen, B. Moussian (eds.), *Extracellular Composite Matrices in Arthropods*,
DOI 10.1007/978-3-319-40740-1_12

substances. Perhaps, one of the best-characterized fibers represented is cocoon silk, which is derived from the domesticated silkworm, *Bombyx mori*. Cocoon silks are composed of two core silk proteins along with an outer adhesive protein known as sericin. Scientists can obtain 300–1200 m of usable fiber from a single silkworm cocoon after alkaline and heat treatment to remove the sericin layer. As the development of new biomaterials is becoming a pressing need for humanity, the scientific community has focused on exploring potential uses of natural materials that offer a broad range of diverse mechanical properties. Spider silk has outstanding material properties and certain threads, such as dragline silk, outperform Nylon, Kevlar, and high-tensile steel with respect to strength and toughness (Gosline et al. 1999). Spiders spin a plethora of different silk types with unique mechanical properties, having evolved specialized abdominal biofactories or silk-producing glands to synthesize structural proteins known as fibroins. New methodologies are emerging for large-scale production of recombinant fibroins, processing, and extrusion of fibers via mimicking conditions that resemble natural fiber synthesis, setting the stage for scientists to develop novel biomaterials. Throughout history, spider silk has served as materials for gill and dip nets, fishing lures, and ceremonial dresses. In fact, ancient Australian aborigines and natives of New Guinea have utilized spider silk as fishing lines, head gear, and bags (Lewis 1996). Spider silk has also been used for crosshairs in a number of different optical devices, including microscopes, telescopes and guns due to its small diameters (Lewis 1996; Gerritsen 2002). Additionally, in medieval and Roman times, people have used cob-webs as bandages to wrap wounds and promote wound healing, a property largely due to the unique biochemical characteristics of spider silks (Bon 1710). These properties include biocompatibility, slow degradability, and high tensile strength. More recently, spider silk has been utilized as artificial supports for nerve generation (Allmeling et al. 2006). Although the Chinese have harvested cocoon silk from silkworms for over 5000 years, spider silks are not readily attainable through conventional farming practices. Spiders are cannibalistic in nature, venomous, and "milking" these organisms to collect fibers on large-scale formats is impractical. Because of these barriers, scientists have turned to the utilization of recombinant DNA methodologies to clone spider silk genes for expression in a wide range of different organisms. The black widow spider, *Latrodectus hesperus*, a cob-weaver, is rapidly becoming a model organism of arachnids for the study of spider silk synthesis and extrusion. The long-term goal for scientists is to manufacture large quantities of artificial spider silk fibers for a variety of diverse applications, including medicine, engineering, and defense. In this book chapter, we will explore the diversity of spider silks and fibroins, their natural extrusion process, the systems that have been used for heterologous expression of recombinant spider silk proteins, and synthetic spinning techniques.

## 12.2 Diversity of Spider Silk

### *12.2.1 Different Spider Silk Glands*

Over 300 million years of natural selection, spiders have evolved different silk-producing glands that have become quite specialized in synthesizing different fibroins or spidroins (a contraction of the words spider and fibroin). These spidroins can be spun into fibers that exhibit diverse mechanical properties, providing important biological functions that are critical for survival in the environment. Each gland is equipped to produce fibers with specialized functions and the resultant fibers serve important and distinct roles including locomotion (dragline silk), prey wrapping (aciniform silk), protection of eggs (tubuliform and aciniform silks), prey capture (dragline and aggregate glue silk) and web construction (dragline and attachment disc silks; Table 12.1). Based upon ecological and histochemical studies, the primary roles of the silk-producing glands are (1) synthesis of spidroins and glue components; (2) transport of silk proteins out of the cells; (3) production of proteins that prevent spidroin and glue component degradation while stored in the storage component; (4) assembly and extrusion of the materials.

Through microdissections and histological studies, the scientific research community has advanced its knowledge of the morphological features of the silk-producing glands, revealing that these structures have quite distinct physical appearances. Anatomical studies support that black widow spiders contain 7 distinct silk-producing glands, including the major and minor ampullate glands (MA and MI), tubuliform (TB), aciniform (AC), pyriform (PY), flagelliform (FL) and aggregate glands (AG; Fig. 12.1). Each gland has its own tubing or "hose-like" structures that allow the liquid spinning dope to be extruded as materials exit from the spinneret. Thus, an individual spider can extrude multiple silk types simultaneously, allowing the spider to produce a host of different composite materials.

**Table 12.1** Different silk-producing glands and biological functions of the extruded fiber types from orb- and cob-weavers

| Silk type and biological function | |
|---|---|
| Silk type | Function |
| Major ampullate | Locomotion, web frame, scaffolding fibers, gumfoot lines |
| Minor ampullate | Prey wrapping, temporary spiral capture silk |
| Flagelliform | Secretion of materials to prevent web degradation, major constituent of capture spiral |
| Aciniform | Prey wrapping, protection of eggs |
| Tubuliform | Protection of eggs |
| Aggregate | Adhesive droplets on gumfoot lines |
| Pyriform | Fastening dragline silk and joining scaffolding fibers |

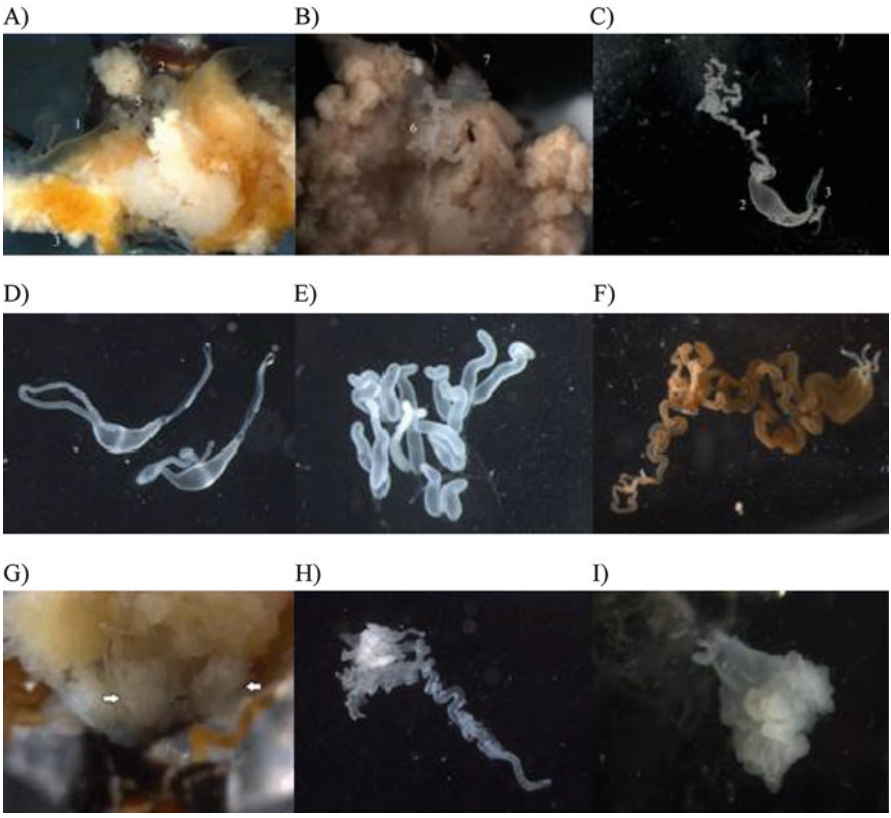


**Fig. 12.1** Different silk-producing glands from a female black widow spider after microdissection. (**a**) Five of the seven silk-producing glands are shown; glands are 1 = MA; 2 = MI; 3 = TB; 4 = AG; 5 = FL; (**b**) Two of the seven silk-producing glands; glands are 6 = AC; 7 = PY; (**c**) MA gland; (**d**) MI gland; (**e**) AC gland; (**f**) TB gland; (**g**) PY gland; (**h**) FL gland; (**i**) AG gland

### *12.2.2 Morphological Features of the Silk-Producing Glands*

Most research to date has been conducted on the major ampullate (MA) gland, largely because its characteristic ampulla shape and enormous size relative to other silk-producing glands make it easy to identify during dissections. Anatomical studies reveal the MA gland consists of three regions: a tail, ampulla, and spinning duct (Fig. 12.1c). Specialized epithelial cells are found in the tail region, functioning to manufacture and secrete vast quantities of dragline silk proteins. These spidroin proteins are then stored as a spinning dope in the ampulla, a bulb-like structure. The concentration of the spinning dope can approach 30 % weight/volume (w/v) in the ampulla. As the liquid is pushed into the spinning duct, which is a long S-shaped structure, it undergoes a phase transition into a solid material.

The minor ampullate (MI) gland resembles the morphology of the major ampullate gland, but it is smaller in appearance (Fig. 12.1a). Both MA and MI glands are whitish in color and found in pairs within an individual spider (Fig. 12.1c–d). Tubuliform glands, which are often pigmented, such as an orangish coloration in *L. hesperus* female species, are present as two sets of three (6 tubules) and are long cylindrical structures (Fig. 12.1f). Aciniform glands resemble small "hot-dog" shaped structures and are found in clusters, also displaying a whitish appearance (Fig. 12.1e). The flagelliform and aggregate glands are often intertwined in the abdomen of the spider, and share somewhat similar morphological features and transparent coloration (Fig. 12.1h–i). Lastly, the pyriform gland, which is pear-shaped and whitish in color, is one of the most difficult glands to remove as an intact structure due to its multiple lobules (Fig. 12.1b, g) (Jeffery et al. 2011). Histochemical analysis reveals that the pyriform gland has two distinct parts called the excretory duct and the secretory sac, which contains two unique secretory cell types (Kovoor and Zylberberg 1980; Kovoor and Zylberberg 1982). Dissection of the pyriform gland followed by isolation of intact RNA has been a challenging task for many labs across the globe. Aside from the major and minor ampullate glands, the other five silk-producing glands have distinct morphological characteristics (Fig. 12.1).

### *12.2.3 Different Silk Types and Biological Functions*

Dragline silk has been extensively studied at the molecular and mechanical level. It is commonly known as a "safety line" for spiders because this fiber type is extruded when they fall from their webs, serving as the principle fiber type for locomotion. Spiders drop from webs by extruding dragline silk, which is cemented to the web by secretion of pyriform silk (Fig. 12.2a). Pyriform silk, which forms attachment discs, is comprised of small diameter fibers that are extruded in an adhesive substance that dries quickly and fastens dragline silk to web fibers, concrete, wood, glass, plant materials, and other abiotic and biotic materials (Blasingame et al. 2009; Geurts et al. 2010a). Black widow spiders also utilize dragline silk for web construction in three different locations: the web frame, scaffolding, and gumfoot lines. Scaffolding fibers constitute the majority of the web and are interconnected in a three-dimensional manner (Fig. 12.2b). Gumfoot lines are threads that run in a vertical fashion. These fibers are attached to the scaffolding of the web and the ground and are coated with glue droplets (Fig. 12.2c). Constituents of the glue droplets are likely derived from the aggregate gland, serving to enhance prey capture (Blackledge et al. 2005).

The precise biological function of minor ampullate silk is unknown in cob-weavers. One study, however, has reported crickets being wrapped with MI silk suggesting that it plays a role in prey wrapping similar to aciniform silk (La Mattina et al. 2008). In addition to prey wrapping, aciniform silk appears to be involved in the protection of eggs, being spun and interweaved with tubuliform silk to form egg sacs (Fig. 12.2e) (Hayashi et al. 2004; Hu et al. 2005b; Vasanthavada et al. 2007).

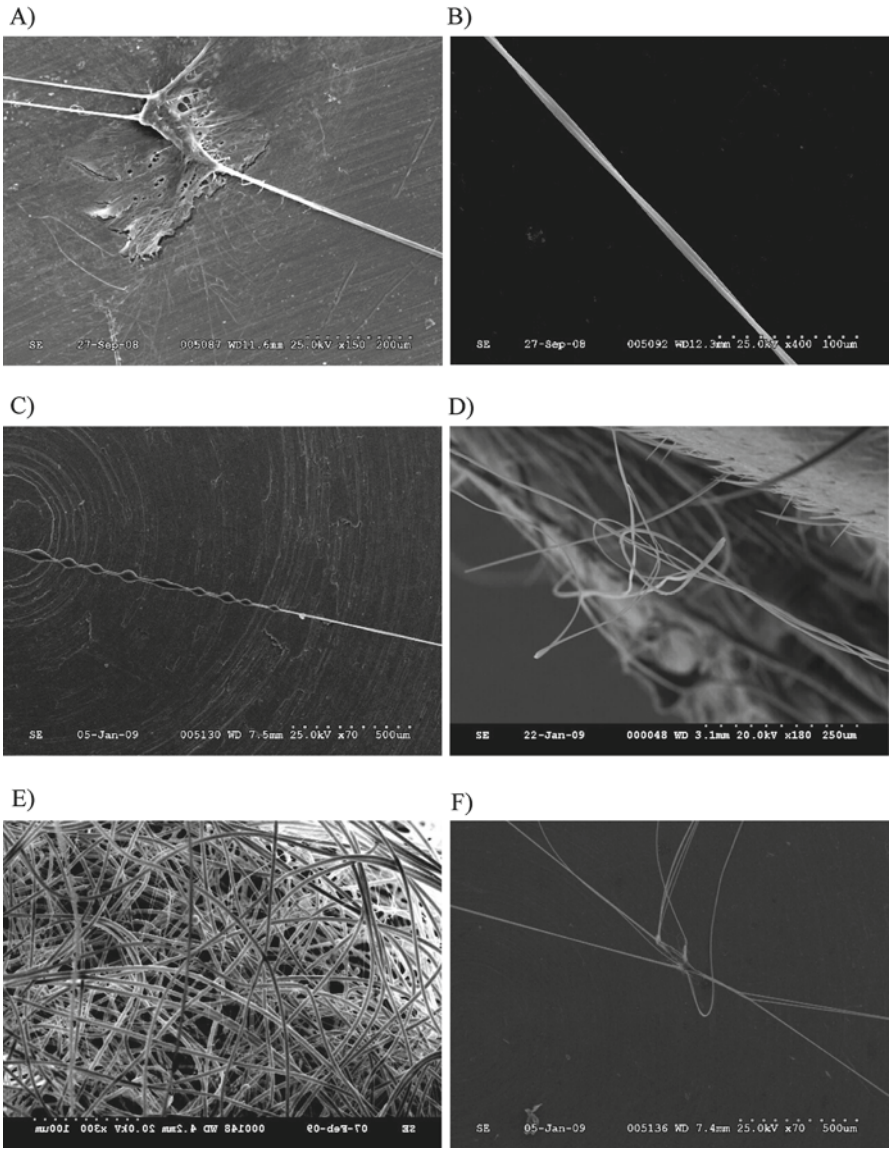


**Fig. 12.2** SEM images of different fiber types spun by the black widow spider. (**a**) Pyriform silk in attachment discs; (**b**) Scaffolding silk; (**c**) Glue droplets on a gumfoot thread; (**d**) Wrapping silk on a cricket; (**e**) Egg sac (tubuliform and aciniform); and (**f**) Connection joints

Aciniform fibers have diameter sizes that are approximately 500 nm, while tubuliform threads are an order of magnitude larger, having diameter sizes of 5 μm (Vasanthavada et al. 2007). Egg sacs represent the easiest silk type to collect from female spiders; egg sacs are largely comprised of tubuliform silk (Fig. 12.2e). In orb-weavers, the flagelliform gland has been shown to extrude spiral capture silk.

Since the webs of black widow spiders lack spiral capture threads, this fiber type appears to be absent, raising the question regarding the function of the flagelliform gland in cob-weavers. As data continues to surface, it appears that the flagelliform glands function in black widow spiders to extrude peptides that coat scaffolding fibers, egg cases, attachment discs, and gumfoot lines to function as antimicrobial agents, likely slowing down web degradation in the natural environment.

### *12.2.4 Genes and Spidroins*

In the past few years, full-length gene sequences have been reported for a number of spidroin family members, including the major ampullate spidroins (MaSp1 and MaSp2), minor ampullate spidroin (MiSp), aciniform spidroin (AcSp1), and tubuliform spidroin (TuSp1) (Table 12.2) (Ayoub et al. 2007, 2013, Chen et al. 2012). Partial cDNA sequences coding for pyriform spidroins (PySps) and other proteins identified in the different silk types have been reported as well (Blasingame et al. 2009; Perry et al. 2010). Similar to other structural proteins that are found in nature, the basic spidroin architecture can be summarized as consisting of internal block repeat modules that are flanked by non-repetitive N- and C-terminal domains (NTD and CTD). For example, the central domains of MaSp1 and MaSp2 are composed of approximately 100 tandem copies of internal block repeats that are 25–35 amino acids in length and are flanked by highly conserved non-repetitive N- and C-terminal domains (Table 12.3) (Ayoub et al. 2007). Spidroin family members are distinguished by having differences in their internal block repeat modules. These differences include having variable lengths and different amino acid compositions specific to each spidroin member. The NTD and CTD, which are both approximately 100 amino acids long, are highly conserved at the amino acid level between spidroin family members, suggesting these domains serve important biological functions during the spider silk assembly pathway (Fig. 12.3a–b). The NTD includes a secretion signal that is removed in the processed, secreted spidroin (Fig. 12.3a). NMR studies of recombinant NTD and CTDs expressed and purified from bacteria

**Table 12.2** Different silk-producing glands and spidroins and other silk proteins extruded from the glands

| Different silk glands and spidroins | |
|---|---|
| Silk gland | Fiber proteins |
| Major ampullate | MaSp1, MaSp2, AcSp1, CRPs |
| Minor ampullate | MiSp1 |
| Flagelliform | SCP-1, SCP-2 |
| Aciniform | AcSp1 |
| Tubuliform | TuSp1, ECP-1, ECP-2 |
| Aggregate | AgSF1, AgSF2, ASG2 |
| Pyriform | PySp1 |

**Table 12.3** Comparison of the ensemble repeats and core units in *L. hesperus* spidroin family members

| Silk | Ensemble Repeats | Core Units | Size (aa) |
|---|---|---|---|
| MaSp1 | GGAGQGGQGGYGRGGYGQGGAGQGGAGAAAAAAAA (Type 1)<br>GGAGQGGQGGYGQGGYGQGGAGQGGAAAAAAAA (Type 2)<br>GGAGQGGYGRGGAGQGGAAAAAAA (Type 3)<br>GAGQGGYGGQGAGQGGAGAAAAAAAA (Type 4) | GGX<br>$(A)_n$; n = 7 | 25-35 |
| MaSp2 | GGAGPGRQQAYGPGGAGAAAAAAAAA (Type 1)<br>GPGPSGYGPGAAGPSGPGLAGAAAAAAA (Type 2)<br>GGSGPGGYGQGPSGYGPSGPGGQQGYGPGGSGAAAAAAAAA (Type 3)<br>GGPGYGGQQGYGPGGAGAAAAAAA (Type 4) | GGX<br>$(A)_n$; n = 7<br>GPGXX<br>QQ | 24-41 |
| MiSp1 | GAGGYGQGAGGYGQGQGAGAGAGAGAGA | $(GA)_n$ | 23 |
| AcSp1 | QLASGIVLGVSTTAPQFGVDLSSINVNLDISNVARNMQASIQGGPAPITA<br>EGPDFGAGYPGGAPTDLSGLDMGAPSDGSRGGDATAKLLQALVPALLK<br>SDVFRAIYKRGTRKQVVQYVTNSALQQAASSLGLDASTISQLQTKATQ<br>ALSSVSADSDSTAYAKAFGLAIAQVLGTSGQVNDANVNQIGAKLATGIL<br>RGSSAVAPRLGIDLSGINVDSDIGSVTSLILSGSTLQMTIPAGGDDLSGGY<br>PGGFPAGAQPSGGAPVDFGGPSAGGDVAAKLARSLASTLASSGVFRAA<br>FNSRVSTPVAVQLTDALVQKIASNLGLDYATASKLRKASQAVSKVRMG<br>SDTNAYALAISSALAEVLSSSGKVADANINQIAP | GGX<br>$(S)_n$<br>$(A)_n$; n = 2 | 376 |
| TuSp1 | GVGASPFQYANAVSNAFGQLLGGQGILTQENAAGLASSVSSGISSAASS<br>VAAQAASAAQSSAFAQSQAAAQAFSQAASRSASQSAAQAGSSSTSTTT<br>TTSQAASQAASQSASSSSSAASQSAFSQASSSALASSSSFSSAFSSASSAS<br>AVGQVGYQIGLNAAQTLGISNAPALADAVSQAVRTV | $(S)_n$<br>$(A)_n$; n = 2 | 184 |
| PySp1 | AAAQAQAETRARAEAVARAQAQAEARVRAEAAARAQAQAEAAARAQ<br>AQAEAAARAQAQAEAAARAQAQAEAAARAQAQAEAAARAQAQAEA<br>AARAQSQSEAAARAQAQAEAAARAQAQVEAAARAQAQAEAAARAQA<br>QAEARAKAEAAVRAQAQVEAAARAQAQVEAAARAQAQAEAAARAQ<br>AQAEARAKAEAAARAQAQAEARAKAEATARAKAQAEAAARAQAQAE<br>ARAIAEAAARAQAQAEARAKAEAAARAQAQAIARAEAAARAQAEAEA<br>RAYAEALARVQAEAATRAQAQTQSRTQAVTHSHAHSASHASSQASSET<br>YAESTAHTATETHEHTSSHSQTASHSQAASHSKAKAHTEADTYSQAQS<br>AAHTI | RAQAQAE<br>$(A)_n$; n = 3 | 376 |

reveal three-dimensional structures that are similar, having a five-helix bundled structure (Hagn et al. 2010; Parnham et al. 2011). In MaSp1 and MaSp2, the CTD forms a parallel-oriented dimeric five-helix bundle and is stabilized through the formation of an intermolecular disulfide bond between a conserved cysteine residue that resides within helix 4 of the monomer (Hagn et al. 2010). SDS-PAGE analysis of recombinantly expressed proteins in bacteria has shown that dimeric complexes are present under oxidizing (non-reducing) conditions, supporting the importance of the cysteine residue in protein dimerization and spidroin aggregation. Site-directed mutagenesis of the cysteine to a serine within the MaSp1 CTD was also shown to eliminate dimerization and affect fiber formation, further supporting the critical role of the cysteine residue and the assembly process (Fig. 12.3b) (Ittah et al. 2007). The stability of the NTD and CTDs and solubility is regulated by the formation of protons and $CO_2$ generated by carbonic anhydrase (Andersson et al. 2014).


**Fig. 12.3** Alignment of the conserved non-repetitive domains of *L. hesperus* spidroin family members. (**a**) N-terminal domain (NTD); (**b**) C-terminal domain (CTD). *Asterisk* represent identical residues; *single* and *double dots* represent amino acids with similar properties. N-terminal section signals or conserved Cysteine residues are shown in *bold text*

### 12.2.5 *Transcriptomic Analysis of the MA Gland and Proteomic Analysis of Dragline Silk*

MA silk is the silk type most thoroughly characterized and studied silk type by the scientific community. During the early 1990s, scientists started to unravel the molecular constituents of MA silk from the golden orb weaver spider, *Nephila clavipes*. By solubilizing MA silk followed by proteolytic digestion, and then sequencing of the peptide fragments using the Edman degradation procedure, investigators were able to obtain MA spider silk gene sequences. These peptide sequences were used to generate DNA probes to screen a cDNA library prepared from MA tissue. This led to the identification of partial cDNA sequences for MaSp1 and MaSp2, the two main protein constituents of MA fibers (Xu and Lewis 1990; Hinman and Lewis 1992). Subsequent studies have led to the retrieval of these full-length genomic DNA sequences and their regulatory sequences from *L. hesperus* (Ayoub et al. 2007). Each gene consists of a single enormous exon (>9000 base pairs), coding for polypeptides that are highly repetitive and masses that exceed 250-kDa. Glycine and alanine residues represent more than 64 % of the amino acids in the spidroin protein sequences (Fig. 12.4a–b). Both glycine and alanine codons are GC-rich, consisting of GGN and GCN triplets, respectively. At the wobble position of the codons there is a biased nature for adenine (A), which likely serves an important role to reduce GC-rich secondary structure in the large MaSp1 and MaSp2 mRNA transcripts, which can exceed 10 kilo-bases.

Chromosome mapping of dragline silk genes using fluorescent *in situ* hybridization has revealed 3 copies of the MaSp1 gene and a single copy of the MaSp2 gene in the spider genome of *L. hesperus* (Zhao et al. 2010). Analysis of the primary sequences of the spidroins has shown that they are highly modular in their architecture. MaSp1 and MaSp2 contain internal block repeats that consist of poly-alanine domains [poly-(A)/GA] and glycine-rich domains, and in the case of MaSp2, it also contains Gly-Pro-Gly (GPG) motifs. These GPG motifs have been proposed to form type II beta-turns, playing an important role in the extensibility of dragline silk. The internal block repeats are about 24–41 amino acids in length (Table 12.3). Sequence comparisons of MaSps from other species revealed the poly-alanine regions consist of 4–7 alanine residues and the X position is commonly occupied by Q, Y, or L in the GGX segments (Ayoub et al. 2007). The complete genetic blueprints for MaSp1 (one of the three loci) and MaSp2 were published for *L. hersperus* (Ayoub et al. 2007). Similar to *N.* clavipes, these blueprints showed that MaSp1 and MaSp2 also consist of one large exon that translates into a highly repetitive polypeptide. The 5′ and 3′ ends of the exon code for the non-repetitive conserved N- and C-terminal domains, respectively. MaSp1 was demonstrated to contain four types of ensemble repeat units that can be iterated up to 20 times, with each one consisting of a glycine-rich region followed by a poly-A region (Table 12.3; sizes are 25–35 amino acids). The repetitive region of MaSp2 has also been characterized to consist of four types of ensemble repeat units, but these repeat units show more variability relative to

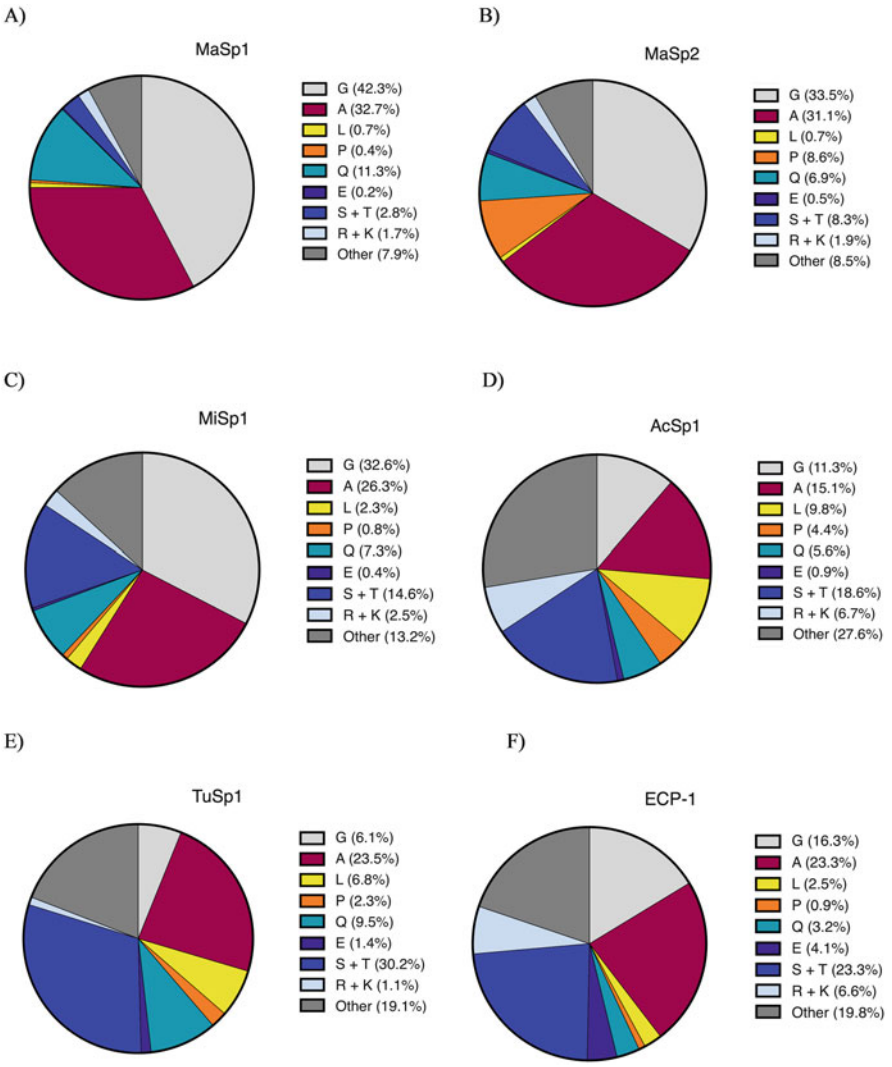


**Fig. 12.4** Predicted amino acid composition of spidroins and ECP-1 from *L. hesperus*. (**a**) MaSp1; (**b**) MaSp2; (**c**) MiSp1-like; (**d**) AcSp1; (**e**) TuSp1; and (**f**) ECP-1. Amino acid percentages (e.g. G, A, L etc.) can be read in a *clockwise* fashion

MaSp1 (Table 12.3). In addition, the ensemble repeats for MaSp2 are not always strung together in the same order.

Transcriptome studies from *L. hesperus* have identified 647 silk gland-specific transcripts (SSTs), including mRNAs coding for silk fiber components, as well as proteins involved in oxidation-reduction, protein degradation, and somewhat paradoxically, inhibition of protein degradation (Clarke et al. 2014). Seventy-five percent of the SSTs were not able to be assigned a functional annotation by an

association with a Gene Ontology (GO) term. Twenty-five percent of the GOs assigned to the SSTs reveal enrichments for proteins involved in oxygen-related functions, including oxidoreductases, oxidation-reduction, monooxygenase, iron ion binding, heme binding, and choline dehydrogenase. There were also elevated SST levels for peptidase inhibitors and peptidases. The presence of peptidase inhibitors could serve to protect the spidroins against protein degradation, while the proteases could be used to degrade all non-exported or improperly synthesized spidroins. Included in the transcriptome list were families for aggregate gland silk factor 2 (AgSF2), aggregate spider glue 2 (AgSG2), ECP-1, and glycine-rich proteins that have no well-defined annotation. Potential orthologs of the capture spiral protein, Flag, which has not been discovered in black widow fibers, were also discovered in the multi-tissue transcriptome analysis (Clarke et al. 2014).

Interestingly, in a different study using massively parallel signature sequencing (MPSS) to profile mRNA expression patterns of the MA gland and cephalothorax (fused head-body) of *L. hesperus*, elevated TuSp1 transcripts were unexpectedly detected in the MA gland. However, no studies have shown that the translated products are spun into MA fibers, suggesting that TuSp1 transcripts are subject to negative translational regulation in the MA glandular tissue (Lane et al. 2013). All three MaSp1 loci are transcriptionally active and detailed analysis of the 3′ UTRs reveal that these molecules undergo alternative polyadenylation. When comparing MaSp1 loci transcript levels, loci 2 was approximately 4 times more abundant relative to loci 1 and 3, supporting that loci 2 is responsible for the dominant product in female black widow spiders. When quantifying MaSp1 and MaSp2 levels, MPSS studies have revealed 3:1 ratios of MaSp1 to MaSp2, which is consistent with the amino acid composition profiles of dragline silk from *L. hesperus* (Casem et al. 1999; Ayoub et al. 2007). Somewhat surprisingly, among the most highly expressed genes in the MA gland that could be annotated were predictions for fasciclin, elongation factor 1-alpha, and lectin (Lane et al. 2013). In addition, at least two different genes encoding transcription factors were also shown to have elevated expression in the MA gland. One of these products was previously identified and shown to belong to the basic helix-loop-helix (bHLH) family of transcription factors. This factor was dubbed Silk Gland Subset Factor (SGSF) based upon its expression pattern in a subset of the silk-producing glands in cob-weavers (Kohler et al. 2005). Members of this family are known to regulate important processes such as cellular proliferation, differentiation, and neurogenesis. The biological function of SGSF in spiders is currently unknown, but electrophoretic mobility shift assays (EMSA) have shown that SGSF is capable of binding to the consensus sequence CANNTG (N = any nucleotide), also known as an E-box site, when it dimerizes with class I bHLH members, such as Daughterless (Kohler et al. 2005). Because DNA sequence analysis of the MaSp1 and MaSp2 promoter regions reveals the presence of conserved E-boxes, it is intriguing to speculate that SGSF, given its elevated expression pattern in the MA gland, could participate in the transcriptional regulation of the dragline silk genes (Ayoub et al. 2007).

MS/MS studies performed on solubilized dragline silk subject to in-solution tryptic digestion have confirmed the presence of MaSp1 and MaSp2 in the fibers of

*L. hesperus*. At the same time, these have failed to detect peptides derived from TuSp1 (Pham et al. 2014). Collectively, these studies support the TuSp1 transcript detected by the transcriptome analysis of the MA gland is subjected to translational regulation. During this same analysis, a new family of low molecular weight cysteine-rich proteins (CRPs) were also shown to be major constituents of the fibers (Pham et al. 2014). In addition, a more recent proteomic analysis of the major and minor ampullate glands, along with the tubuliform gland from *L. hesperus* was reported (Chaw et al. 2015). These studies have confirmed the presence of the CRPs in the spinning dope of the MA gland and, somewhat surprisingly, the presence of a previously characterized spidroin from the aciniform gland, AcSp1. At this point in time, it is unclear of the role of AcSp1 in dragline silk which warrants further investigation. Several other proteins were also identified in the MA gland, including aggregate spider glue 2 (AgSG2), alpha-2 macroglobulin (A2M), carboxylic ester hydrolase (CEH), dimethylaniline monooxygenase (FMO3), and a putative triacylglycerol lipase (PTL) (Chaw et al. 2015). Although the precise role of these other constituents is unclear, it would appear they play an important role in the silk assembly pathway.

### *12.2.6 Minor (MI) Ampullate Silk*

In contrast to MA silk proteins, solution state conformational studies using Fourier transform infrared spectroscopy (FTIR) with deuterated-labeled MI silk proteins reveal a significant fraction of α-helical structure and reduced beta-sheet structure (Dicko et al. 2004a). Moreover, solid-state NMR studies performed on MI fibers support that the conformation of alanine residues are more heterogeneous when compared to alanine residues in MA silk, displaying a larger fraction of alanine residues in a non-beta sheet conformation (Liivak et al. 1997). Several research groups have characterized the mechanical behavior and microstructure of orb-weaver MI silk. Despite over 100 million years of divergence, different species show similarities in their mechanical properties of MI silk. Tensile tests demonstrate that MI fibers exhibit similar breaking stress values relative to MA fibers. However, when these fibers are submerged in water, dried, and subjected to mechanical testing, MA and MI fibers behave differently. The plasticizing effect of water on MA fibers is much stronger, showing a three order of magnitude reduction in the initial elastic modulus after exposure to water (Guinea et al. 2012). In this manner, MI silk does not show a supercontraction effect and its behavior in water is more similar to *B. mori* silk. Because MI silk does not exhibit supercontraction when placed in water, it has advantages over MA silk for biomedical applications or processes that cannot tolerate structural changes due to humidity or increased aqueous environments. SEM analyses of fibers collected from *Nephila inaurata* and *Argiope trifasciata* reveal mean diameter sizes of 1.8 μm (Guinea et al. 2012), which is smaller relative to diameter sizes of MA fibers.

By using a multidimensional PCR approach, the full-length gene sequence of MiSp1 from the orb-weaver *Araneus ventricosus* was shown to consist of two exons and a single intron (Chen et al. 2012). The predicted transcript length is 5440 bases, encoding a protein that contains 1766 amino acid residues. Similar to other spidroin family members, the architecture of MiSp1 is organized into non-repetitive N- and C-terminal domains and a predominantly repetitive region composed mainly of glycine and alanine (Fig. 12.4c). *A. ventricosus* MiSp1 contains more sequence and length variation within its internal block repeats (repetitive regions) than *L. hesperus* MaSp1. The repetitive region of MiSp1 is comprised of three distinct regions; these regions are referred to as region I, II, and III. The poly-Ala (A) motif occurs frequently within region I, but it is the most frequent in region III (the longest region), where it appears 8 times. These repetitive regions consist of 4 types of motifs: GX (X = A, Q, I, V, E, S, and D), GGX (X = A, S, V, E, and Y), GGGX and short poly-A repeats. Although the poly-A repeats are longer and more abundant in MaSp1 primary sequences, $(GA)_n$ motifs are more highly represented in MI spidroins. It has been hypothesized that the $(GA)_n$ iterations, similar to poly-A blocks, form beta-sheet structures in the silk (Hayashi et al. 1999). Region I and II, as well as region II and III, are interrupted by two spacer regions that are serine-rich. The spacer regions are predicted to form alpha-helical structures. Kyte and Doolittle hydropathy profiles predict an alternating profile of hydrophobicity (poly-A motifs) and hydrophilicity (glycine-rich regions) for *A. ventricosus* MiSp1 over its entire sequence (Chen et al. 2012). Somewhat surprising, despite the close evolutionary relationship, the *A. ventricosus* MiSp1 repetitive region is different from sequences reported from translated partial cDNAs from MiSp1 and MiSp2 of *N. clavipes* (Colgin and Lewis 1998). Several other labs have published partial cDNA sequences for MiSps or MiSp1-like molecules, including nucleic acid sequences from cob-weaver spiders (Table 12.3) (Gatesey et al. 2001; La Mattina et al. 2008). In orb-weavers, MiSp1 is spun into temporary spiral capture silk, whereas in cob-weavers, it has been shown to be present within silk collected from wrapped crickets (La Mattina et al. 2008).

Analysis of the N-terminal domain of *A. ventricosus* predicts five alpha helices, which is similar to the solution-state conformation determined by NMR using the NTD of recombinant MaSp1 (Parnham et al. 2011). There are two cysteine residues that reside within helix 1 and 4 of the *A. ventricosus* MiSp1 NTD that are well conserved in the NTDs of TuSp1, CySp1, MaSp2 and MiSp1, suggesting that these residues participate in the formation of an intradisulfide linkage. When analyzing the C-terminal domain of *A. ventricosus*, glycine, alanine, serine and valine represented 64 %. In contrast to most other domains, cysteine was absent in the *A. ventricosus* MiSp1 C-terminal domain.

### 12.2.7 Aciniform Silk

Spiders use this silk type for wrapping prey, building sperm webs, producing web decorations, and for constructing egg sacs (Hu et al. 2006b). Thus far, biochemical studies support that aciniform silk consists of a single protein, aciniform spidroin 1 (AcSp1) (Hayashi et al. 2004; Vasanthavada et al. 2007). Full-length and partial cDNAs coding for AcSp1 or AcSp1-like molecules have been reported in the scientific literature. Analysis of the full-length cDNA sequence from *Argiope trifasciata* reveals 14 copies of internal block repeat modules that are highly homogenous. AcSp1 internal block repeats have lengths that are approximately 200 amino acids, which are considerably longer relative to ensemble repeats found within the protein chains of MaSp1 and MaSp2. However, in *L. hesperus* these block repeats are 376 amino acids (Table 12.3). Non-repetitive N- and C-terminal domains are present within the AcSp1 primary sequence. However, using the protein sequence of the AcSp1 CTD, phylogenetic analysis supports it is more evolutionary divergent relative to major and minor ampullate and flagelliform silk proteins (Hayashi et al. 2004). Moreover, translation of the AcSp1 cDNA sequence shows that the amino acid composition is substantially lower in glycine and alanine content relative to the dragline silk fibroins (Fig. 12.4d). Despite the lower levels of glycine and alanine, mechanical testing on aciniform silk reveals these fibers display higher toughness values (ability to absorb more energy per unit volume without failing) relative to major and minor ampullate silk (Hayashi et al. 2004).

Raman spectra of the luminal content from aciniform glands reveal that *N. clavipes* AcSp1 adopts a 50 % alpha-helical state in solution, but during extrusion the protein chain undergoes a conformational transition. After extrusion, the secondary structure of AcSp1 displays 24 % alpha-helical and 30 % beta-sheet structures in the solid fibers (Lefevre et al. 2011). Solution-state NMR spectroscopy has been used to investigate the atomic-level structure of the internal block repeat recombinant AcSp1 from *A. trifasciata*. In these studies, a 199 residue repeat unit (called $W_1$; lacks CTD) was demonstrated to have a well-folded, tightly packed ellipsoidally-shaped helical core in solution from amino acid residues 12–149, flanked by unstructured N- and C-terminal tails (Tremblay et al. 2015). The tightly packed ellipsoidally-shaped helical core consists of a 5-helix bundle structure. This structure was shown to have high thermal stability and can undergo reversible denaturation at 71 °C. Under near-physiological conditions it can also form self-assembled nanoparticles (Xu et al. 2013).

### 12.2.8 Tubuliform Silk

Female spiders manufacture tubuliform silk and use it to construct egg sacs to help protect their offspring during development. It is typically manufactured during the reproductive season. Partial cDNA sequences coding for the main constituent of

tubuliform silk, tubuliform spidroin 1 (TuSp1), have been reported from orb-weavers *Argiope aurantia*, *Araneus gemmoides* and *Nephila clavipes* (Tian and Lewis 2005). In addition, partial cDNAs coding for TuSp1 in the cob-weaver, *L. hesperus*, has been isolated by cDNA library screens (Hu et al. 2005b). Analysis of the primary amino acid sequences of TuSp1 reveals that it lacks common silk modules that are present within major and minor ampullate fibroins (e.g. GGX, GPGXX, poly-A, and spacer regions). Instead, it shows a complex architecture with distinct motifs embedded within 184 ensemble block repeat segments, including $S_n$, $(SQ)_n$ and GX (X represents Q, N, I, L, A, V, Y, F or D) (Table 12.3) (Hu et al. 2005b; Tian and Lewis 2005). Relative to MaSp1 and MaSp2, TuSp1 has lower amounts of Gly and Ala, but higher levels of Ser and Thr (Fig. 12.4e). Somewhat unexpectedly, the MaSp1 and MaSp2 transcripts have been detected in tubuliform glands of *L. hesperus*, but no MaSp1 or MaSp2 protein constituents have been reported within egg sacs. Full-length cDNA sequences for TuSp1 have been reported for the orthologs CySp1 and CySp2, two silk proteins that are manufactured by the cylindrical (tubuliform) glands of the wasp spider, *Argiope bruennichi* (Zhao et al. 2006). The C-terminal domain of TuSp1 has been shown to have little, if any, similarity to other silk fibroin family members, suggesting this fibroin represents an evolutionarily ancient silk protein that is spun into tubuliform silk (Garb and Hayashi 2005; Tian and Lewis 2006). Cylindrical and tubuliform glands are identical structures, but in the scientific community the terms are often used interchangeably. Despite the absence of poly-A block repeats in the TuSp1 protein architecture, TuSp1 is still capable of adopting nanocrystallite beta-sheet structures in fibers; the motifs AASQAA, AAQAA, and AAQAASAA have been shown to be responsible for beta-sheet formation (Table 12.3) (Tian and Lewis 2006).

Although TuSp1 is a major constituent of tubuliform silk, two other proteins, Egg Case Protein-1 and 2 (ECP-1 and ECP-2), have been identified by MS/MS analysis of peptide fragments derived from egg cases; these molecules were discovered by solubilizing egg sacs from *L. hesperus* with chaotropic agents, followed by in-solution tryptic digestion (Hu et al. 2005a, 2006a). Similar to MaSp1 and MaSp2, the ECPs contain large amounts of Gly and Ala (Fig. 12.4f). ECP-1 and ECP-2 lack well-defined internal block repeat modules as well as the conserved, non-repetitive NTD and CTDs that are hallmark features of traditional spidroin family members. Additionally, these proteins have lower molecular weights relative to spidroins, with predicted masses of approximately 80-kDa instead of >200-kDa masses that are commonly reported for spidroins. ECP-1 and ECP-2 have highly conserved N-termini, sharing 16 Cys residues found within the first 153 amino acids (Hu et al. 2006a). These N-termini are markedly divergent from the NTD of other spidroin family members. Using recombinant ECP-2 proteins purified from bacteria, synthetic silk fibers were produced by wet-spinning methodologies, supporting these molecules have properties that are fibroin-like. These fibers show comparable mechanical properties relative to synthetic silk fibers produced from recombinant MaSp1 molecules (Gnesa et al. 2012).

### 12.2.9 Pyriform Silk

Pyriform silk was the last fiber type to be characterized at the biochemical level. This fiber type, which is also referred to as piriform silk, is spun from a pear-shaped structure located in the abdomen that exits a short duct opening into a nozzle-like spigot (Kovoor and Zylberberg 1982). Numerous spigots on the spinneret serve to extrude fibers that form a mesh-like structure (Wolff et al. 2015). Pyriform silk serves to fasten dragline fibers to surfaces with a minimum of material consumption, providing a function that is central to spider locomotion. Pyriform silk is secreted into a liquid material that polymerizes rapidly (less than a second) under ambient conditions, forming a structure referred to as an attachment disc. Attachment discs are highly stable structures, capable of surviving in the natural environment for years. Similar to other spider silk types, these structures are biodegradable, biocompatible, and extremely versatile. SEM and biochemical analyses of attachment discs show these structures are coated with a glue-like cement containing nanofibrils enclosed in a presumptive lipid-based material which creates a meshwork organization that facilitates stress distribution and crack arrestment when placed under a load (Geurts et al. 2010b; Wolff et al. 2015). The macroscopic structure of attachment discs is the product of a highly conserved behavioral program that involves precise movement of the abdomen, which generates countless parallel loops of crossing silk threads (Eberhard 2010). It has been reported that an attachment disc from a golden orb-weaver, *Nephila senegalensis*, can hold 4–6 times its body weight when fixed to a glass surface (Wolff et al. 2015). Given the unique design of these biomaterials, the elucidation of the intrinsic composite structure of attachment discs from different spider species has tremendous value for the development and engineering of new nanocomposites that are light-weight in nature.

The proteins that comprise pyriform silk were first reported from the cob-weaver, *L. hesperus* (Blasingame et al. 2009). The major protein constituent was named pyriform spidroin 1 (PySp1) (Blasingame et al. 2009). Shortly following the identification of PySp1 from cob-weavers, a protein with similar biological function was identified from orb-weavers – this molecule was dubbed pyriform spidroin 2 (PySp2) or PiSp1 (Geurts et al. 2010b; Perry et al. 2010). To date, no full-length gene sequences have been published for pyriform spidroins (*PySps*=*PySp1* and *PySp2*), only partial cDNAs are available in the public DNA databases. Translation of the *PySp* cDNAs reveal conventional internal block repeats that are 376 amino acids and a non-repetitive C-terminal domain (Table 12.3). Theoretical amino acid composition analyses of the translated cDNAs, demonstrate these spidroin family members contain the highest quantity of hydrophilic residue content relative to other family members. The high content of polar and charged amino acids likely functions to provide strong interactions between the secretion film and substrate. Undoubtedly, these polar and charged residues within the primary sequences of PySps enhance water-solubility, but also likely serve to direct self-assembly of the fibers. Analysis of the protein sequence of PySp2 demonstrates that the internal

block repeat element has two components: one is classified as a SGA-rich element and the other is proline-rich (P-rich) (Geurts et al. 2010a).

### *12.2.10 Flagelliform Silk*

The major constituent of capture spiral silk in orb-weavers is referred to as the flagelliform (Flag) protein. Capture spiral silk plays a central role to entrap flying prey, serving as an aerial net. Flagelliform fibers are coated with glue material that is extruded from the aggregate gland, a process that facilitates prey capture (Choresh et al. 2009). The aqueous glue provides hydration, which aids in the extensibility of the fibers (Vollrath and Edmonds 1989). From a mechanical perspective the capture spiral represents one of the most elastic materials known and is capable of effectively dissipating the kinetic energy delivered by a prey strike during a collision of an aerial insect. To elucidate how the extensibility of capture silk is related to secondary structure in Flag proteins, translated Flag cDNA sequences have been examined for specific patterns embedded within its protein sequence. Interestingly, Flag proteins are characterized as lacking poly-A motifs, which is a prominent module that contributes to the high tensile strength of MA silk. Despite the absence of poly-A modules, the motifs in the core of the Flag protein sequence include: (1) GPGGX; (2) GGX; and (3) spacer regions (Hayashi and Lewis 1998). In some instances, 63 copies of GPGGX motifs can be found in tandem repeats within the primary sequence of Flag. Iterations of this sequence were proposed to form a β-spiral structure that functions like a nanospring, contributing, in part, to the elastic nature of flagelliform silk. Thus, the molecular mechanism of elasticity is governed by iterations of the GPGGX motifs that form a series of type II β-turns that are linked together in the polypeptide chain. Insight into the biological function of GGX motifs has come from stress-strain studies performed with synthetic fibers spun from purified recombinant proteins. Synthetic fibers spun from recombinant proteins engineered to carry different Flag modules support the GGX motif contributes to extensibility, whereas the spacer region plays a role in the strength of the recombinant fibers (Adrianos et al. 2013).

The role of the flagelliform gland in cob-weavers is controversial, but it appears to have evolved a different ecological function relative to orb-weavers. In the three-dimensional architecture of cob-webs, capture spiral threads are completely absent. Two peptides that are extruded from the flagelliform gland of *L. hesperus* were identified and characterized at the biochemical level. These products were named spider coating peptide 1 and 2 (SCP-1 and SCP-2) (Hu et al. 2007). SCP-1 was shown to have intrinsic metal-binding activity and can be purified from crude protein lysates prepared from flagelliform glands using nickel metal-ion chromatography (unpublished data). Proteomic analyses performed with materials collected from different silk types have revealed the presence of SCPs within attachment discs, egg sacs, scaffolding fibers and gumfoot lines (Hu et al. 2007). Data is emerging to support that SCPs function as anti-microbial agents, helping to protect the

web from degradation. Consistent with this hypothesis is the observation that many microbes require metal ions for survival and proliferation. The ability of SCP-1 to sequester metal ions could attenuate microbial growth and slow web degradation. Collectively, the evolution of compounds that prevent web degradation is consistent with the observation that cob-weavers cast webs and leave them in the environment for prolonged periods of time.

### *12.2.11 Aggregate (Glue) Silk*

Biological adhesives, such as glues, are used by a wide-range of different organisms in the world. Spiders also coat fibers with glue-like substances. In orb-weavers, two glycoproteins were identified in the aqueous glue-like substance that forms the droplets coated on flagelliform silk in *N. clavipes* (Choresh et al. 2009). These proteins have been reported to have unique 110 amino acid repetitive domains that are encoded by opposite strands of the same DNA sequence, but this has not been substantiated by genomic DNA sequencing. Other constituents were discovered in the aqueous solution, revealing its complex chemical composition. In addition to the two glycoproteins, ASG1 and ASG2 (predicted molecular masses are 38- and 65-kDa, respectively), high concentrations of water-soluble organic materials that include free amino acids, small peptides, neurotransmitter-related molecules, as well as low concentrations of inorganic salts were shown to be extruded into the droplets (Vollrath et al. 1990; Tillinghast et al. 1991; Townley et al. 2012). Since cob-weavers lack capture spiral silk, the question arises whether these species produce glue droplets for their webs. Analysis of the three-dimensional webs of *L. hesperus* has revealed the presence of glue droplets at the base of gumfoot lines, which are vertical lines that function as a spring-loaded trap that pulls walking insects into the web (Fig. 12.2c) (Argintean et al. 2006). The adhesion of the droplets serves to immobilize the prey, facilitating the capture of prey. Chemical analyses demonstrate that glue droplets on gumfoot lines from *L. hesperus* are composed of hygroscopic organic salts and glycoproteins, similar to viscid silks (Jain et al. 2015). Although the underlying assumption is that the aggregate gland is responsible for the secretion of this material, a direct linkage of the substances manufactured by the aggregate gland and their extrusion into these droplets remains to be established.

In cob-weavers the aggregate gland was shown to extrude molecules that are constituents of connection joints (Vasanthavada et al. 2012). Connection joints are structures that interconnect more than one fiber (Fig. 12.2f). These structures serve as a structural hub to join scaffolding threads together in the web; these hubs also function to interlock wrapping silk during prey capture. MS/MS analysis of solubilized connection joints led to the discovery of two proteins dubbed aggregate gland silk factor 1 (AgSF1) and aggregate gland silk factor 2 (AgSF2). Western blot anal-

yses also further confirmed the co-localization of the AgSFs to connection joints (Vasanthavada et al. 2012). Inspection of the primary sequences of AgSF1 and AgSF2 reveals different protein architectures compared to traditional spidroin family members. Interestingly, AgSF1 has iterations of the pentameric QPGSF motif, which is an element similar to mammalian elastin. In the case of AgSF2, it has repetitive elements that have the consensus sequence NVNVN. These sequences are embedded in a glycine-rich matrix. More extensive biochemical studies will need to be performed to elucidate the precise interactions and functions of AgSF1 and AgSF2 in the connection joints.

## 12.3 Natural Silk Extrusion Pathway

### *12.3.1 Fiber Extrusion from the MA Gland*

Our understanding of spider silk synthesis, fiber assembly, and the extrusion pathway has been largely derived from studies of the MA gland of the genus *Nephila*. In the abdomen of *N. clavipes*, which has bilateral symmetry typical of orb- and cob-weavers, there are two MA glands that are dedicated for dragline silk production. MA glands have been characterized as having four different zones: the tail region (responsible for synthesis and secretion of the spidroins), the lumen (storage of spidroins), the spinning duct (responsible for the alignment of silk proteins), and the spigot (the nozzle that controls fiber extrusion) (Vollrath and Knight 2001).

The ampulla of the MA gland represents a storage vessel for soluble silk proteins that are manufactured in specialized columnar epithelial cells that reside in the tail region. Using the secretion signal on the N-terminal region of the spidroins, these epithelial cells secrete the spidroins into the lumen. The spidroins are stored in the lumen in a highly concentrated liquid crystalline solution that can approach 30–50 % (w/v) or 300–500 g/L (Vollrath and Knight 2001). Histological studies describe the tail region and ampulla as having two zones, which are named the A-zone and B-zone. Zone A contains a highly elongated and diverging region that consists of tall columnar secretory cells, while zone B represents a converging region characterized by more osmiophilic granules and higher peroxidase concentration (Vollrath and Knight 1999). Following the ampulla is the spinning duct (S-shaped) which has been described as having three limbs (limbs 1, 2 and 3). During the natural spinning process, the spidroins move from the tail region through the spinning duct, where these molecules experience biochemical and physical environmental changes. These changes are accompanied by a liquid-liquid phase separation that is followed by a liquid-solid phase transition that leads to the production of a preliminary silk fiber that further experiences some evaporation of water during the drawdown process of the last limb (limb 3).

### *12.3.2 Models of Spider Silk Extrusion*

The natural spider silk assembly pathway has been described by two different models - the liquid crystalline and micelle-coalescence based theories (Vollrath and Knight 2001; Jin and Kaplan 2003). In the liquid-crystalline theory, the newly synthesized proteins, which are unfolded and rod-shaped, adopt a nematic (thread-like) liquid-crystalline phase. In this phase, the spidroin protein chains are packed in a parallel fashion to each other, but they are perpendicular to the long axis of the tall columnar secretory cells (Vollrath and Knight 2001). As the dope moves through the ampulla, the long axis flips until the packaged structures become parallel with the lining of the epithelial walls. This nematic orientation is maintained until reaching the second limb (limb 2) of the spinning duct, where they are organized into bilayered disks. As the elongational flow and shear forces accelerate in the third limb (limb 3), it leads to the elongation and alignment of the disc-like structures (Vollrath and Knight 1999). During this step, the protein chains undergo a conformational change, transitioning from random coil and polyproline-II helix-like structures to protein folds that have large β-sheet content. Spidroin conformational transitions have also been proposed to be associated with pH changes that occur between the ampulla and spinning duct. The pH was shown to drop from 7.2 to 6.3, triggering spidroins to undergo conformational changes that promote fiber assembly (Dicko et al. 2004b). This conformational change has been proposed to result from the neutralization of a conserved Asp (D) in the NTD of MaSp1, which functions as a pH sensor to control protein assembly (Gaines et al. 2010). Through the combined actions of the chemical and physical events, the spinning dope becomes gelatinous in the distal part of the spinning duct, resulting in increased viscosity. Lastly, in the third limb, the epithelial cells with apical microvilli function to reabsorb water molecules, helping to produce the final fiber product.

In contrast to the liquid-crystalline theory, the micelle theory was largely conceived from the observation that fractured natural silk fibers contain globular structures within their internal core. In order to build a model consistent with the presence of the globular structures and to add clarity to the silk assembly mechanism, synthetic fibers were generated *in vitro* utilizing aqueous solutions of reconstituted silkworm silk fibroins as a spinning dope (Jin and Kaplan 2003). This model of silk assembly proposes that spidroin sequences are amphiphilic in nature. The spidroin molecules contain short alternating hydrophobic and hydrophilic amino acid stretches that are flanked by larger hydrophilic terminal regions that make the proteins surfactant-like, allowing the protein chains to form micelles within the spinning dope material. In these *in vitro* studies, it was shown that by increasing the concentrations of the spidroins, the micelles could coalesce into larger globular structures (Jin and Kaplan 2003). Furthermore, during extrusion, it was proposed that the elongational flow and shear force placed on the liquid due to the ductal wall results in elongation of the globular structures, giving rise to fibrillar morphologies that represent the precursor of the spider silk fiber (van Beek et al. 2002).

For both theories, the proteins passing through the spinning duct experience remarkable changes in the environment of the solvent, resulting in salting-out effects that are associated with the formation of the silk structure. Potassium and phosphate ion concentrations both increase, while there is a decrease in sodium and chloride ion concentration, removal of water, and slight drop in the hydrogen ion concentration (Vollrath et al. 1998; Vollrath and Knight 1999; Knight and Vollrath 2001; Rammensee et al. 2008). Through the eloquent usage of these different chemical and physical processes during extrusion, spiders are capable of spinning a wide-range of diverse threads that are classified as high performance materials. Natural MA silk is renowned for its outstanding material properties. Relative to the tensile strength of steel, the breaking stress of MA silk is comparable, but it is considerably more extensible, leading to a material that is 30 times tougher than steel (Table 12.4) (Gosline et al. 1999). MA silk is also three times tougher than Kevlar, a synthetic fiber that is manufactured in vast quantities by many militaries across the globe during the production of body armor (Table 12.4). In the case of dragline silk, these threads have been shown to have breaking stress and strain values that are approximately 1 GPa and 31 % (Table 12.4) (Hu et al. 2006b). Furthermore, stress-strain curve analyses of different spider silk types reveal a diverse range of mechanical properties that perform well relative to bone, elastin, and carbon fiber (Table 12.4). In the scientific literature, different species of spiders have shown variability with respect to the mechanical properties of their MA silk. Biophysical studies have revealed that MA silk contains a hierarchical architecture where highly organized, hydrogen-bonded β-sheet nanocrystals from the poly-A blocks are arranged within a semiamorphorous matrix that consists of $3_1$-helices and β-turn structures (Kummerlen et al. 1996; van Beek et al. 2002; Lefevre et al. 2007).

**Table 12.4** Mechanical properties of spider silk fibers and other man-made and natural materials

| Mechanical properties of different materials | | | |
|---|---|---|---|
| Fiber | Tensile strength (MPa) | Toughness (MJ/m$^3$) | Extensibility (%) |
| *Araneus* dragline | 1100 | 160 | 27 |
| *Latrodectus* dragline | 996 | nd | 31.1 |
| *Latrodectus* Minor ampullate | 346 | nd | 30 |
| *Latrodectus* Tubuliform | 629 | nd | 71.7 |
| *Latrodectus* Aciniform | 700 | 290 | 80 |
| *Araneus* Flagelliform | 500 | nd | 270 |
| Nylon fiber | 950 | 80 | 18 |
| Kevlar 49 fiber | 3600 | 50 | 2.7 |
| High-tensile steel | 1500 | 6 | 0.8 |
| Bone | 160 | 4 | 3 |
| Elastin | 2 | 2 | 150 |
| Carbon fiber | 4000 | 25 | 1.3 |

*nd* no data for sample

## 12.4 Expression Systems for Recombinant Silk Production

### *12.4.1 Isolation of Spider Silk Genes*

Although the Chinese have been harvesting cocoons from silkworms for thousands of years, farming spiders for large-scale fiber collection is impractical for a variety of reasons. Firstly, spiders are cannibalistic, territorial and venomous – all properties that make them undesirable for domestication. Secondly, the process of "milking" spiders is more challenging and arduous relative to milking cows, making this collection procedure unrealistic, too time consuming, and economically unfeasible. To circumvent the inability to domesticate and farm spiders, researchers have focused on the biotechnological production of recombinant spider silk proteins as alternative strategies. Since silk is largely composed of protein, molecular biologists and protein chemists have embarked on the development of various gene cloning strategies and heterologous expression systems to manufacture enormous amounts of recombinant silk proteins. Because manufacturing spider silk materials requires vast quantities of recombinant spider silk protein for the spinning process, new creative methods to replicate and express spider silk genes in other organisms are being pursued by many companies and research labs across the globe.

For investigators to produce recombinant silk proteins in other organisms, nucleic acid sequences coding for the spidroin family members must be isolated by molecular biological approaches, or alternatively, synthetic pieces of nucleic acids must be designed and assembled into DNA constructs. When the first members of the spidroin family were discovered, labs focused on retrieving spider gene sequences by screening cDNA libraries prepared from silk-producing glands of orb- or cob-weavers by conventional nucleic acid-nucleic acid hybridization (Hinman and Lewis 1992; Guerette et al. 1996; Hayashi and Lewis 2000). Although these library screens were successful, a limitation of the screens was that most of the clones retrieved represented partial cDNA sequences. Moreover, due to the construction of the libraries, most of the partial cDNAs lacked the NTD of the spidroin family members (Gatesey et al. 2001). Despite the availability of other methodologies to clone genes, such as polymerase chain reaction (PCR), the utilization of these techniques was further limited and hampered by the intrinsic properties found within the gene sequences of spidroin family members, which included the presence of repetitive block repeats, their high GC content (Gly and Ala codons), and their incredibly long lengths (>9 kb) (Xu and Lewis 1990; Hinman and Lewis 1992). Collectively, these chemical properties have challenged the reliability and robust nature of PCR to amplify repetitive modules in the fibroin family members as a single intact product. This has forced investigators to screen libraries by conventional methodologies to retrieve cDNAs that have suitable lengths for expression studies. However, as investigators have isolated longer cDNAs from conventional library screens, challenges have surfaced involving basic cloning manipulations of these genes when placed into prokaryotic or eukaryotic backgrounds, including fundamental processes, such as DNA replication and translation. With technology advancing rapidly and the

decreasing costs associated with oligonucleotide synthesis, many research groups and companies are pursuing the synthesis of codon-optimized pieces of single-stranded DNA molecules. These molecules can be annealed and multimerized by seamless cloning strategies to produce artificial spider silk genes that closely resemble natural cDNA sequences (Rabotyagova et al. 2009; Teule et al. 2009).

### *12.4.2 Expression Systems of MA Recombinant Proteins*

Expression studies of recombinant spidroins in prokaryotic and eukaryotic systems have explored a variety of different strategies and approaches, including the utilization of natural spider silk cDNAs, the design of synthetic spider silk genes that are codon-optimized for expression, the implementation of spider gene sequences that are a combination of synthetic and natural cDNA sequences, and the incorporation of cysteine codons into block repeat modules to facilitate disulfide bond formation and crosslinking of recombinant silk protein chains (Table 12.5) (Prince et al. 1995; Grip et al. 2009; Teule et al. 2009). The majority of the expression studies have investigated the production of recombinant silk proteins that represent dragline silk constituents using bacterial expression systems (Table 12.5). In these reports, investigators have induced and purified MaSp1 and MaSp2 molecules, but a large number of these proteins have been truncated recombinant silk proteins. These truncated spidroins have molecular weights that range from 10 to 163-kDa, which is much smaller in mass relative to the native sized spidroin. Additionally, these studies have predominantly centered on the expression of internal block repeat regions, ignoring the incorporation of the highly conserved non-repetitive NTD and CTDs into the recombinant silk proteins. Thus, the synthesis of native-sized spidroins in expression systems has been a challenging barrier to overcome, forcing most investigators to synthesize truncated versions of the silk proteins. One strategy that has led to the production of recombinant silk proteins that approach native-sized spidroins has been achieved using synthetic genes that were expressed in a metabolically engineered strain of *Escherichia coli* designed to manufacture elevated levels of the glycyl-tRNA pool (Xia et al. 2010).

Because amplification of spider silk genes by PCR is difficult due to the repetitive nature of the internal block repeats, new cloning strategies have emerged to synthesize artificial DNA modules. Artificial DNA modules have been constructed from short oligonucleotides repeats that are codon-optimized for high level expression. Multimerization of the oligonucleotide repeats has allowed for fine control over the recombinant protein size. Expression of truncated spidroins, specifically MaSps, has been performed in a variety of different heterologous expression systems, including plants (tobacco and potatoes), yeast (*Pichia pastoris*), and bacteria (*E. coli* and *Salmonella*) (Prince et al. 1995; Lewis et al. 1996; Fahnestock and Bedzyk 1997; Fahnestock and Irwin 1997; Arcidiacono et al. 1998; Fukushima 1998; Winkler et al. 1999; Scheller et al. 2001; Lazaris et al. 2002; Xia et al. 2010). Synthetic genes coding for recombinant proteins ranging from 15 to 250-kDa have

**Table 12.5** Different expression systems, types of spidroin genes expressed, predicted molecular mass, and amount of recombinant protein yielded after purification

| Group | Gene | Protein | Expression system | Size (kDa) | (mg/L)[b] |
|---|---|---|---|---|---|
| *Bacteria* | | | | | |
| Prince et al. (1995) | Synthetic | MaSp1 | *E. coli* SG13009pREP4 | 14–41 | 15 |
| | Synthetic | MaSp2 | | | |
| Lewis et al. (1996) | Synthetic | MaSp2 | *E. coli* BL21 (DE3) | 31/58/112 | 5 |
| Fahnestock and Irwin (1997) | Synthetic | MaSp1 | *E. coli* BL21 (DE3) | 65–163 | 300[c] |
| | Synthetic | MaSp2 | | | |
| Fahnestock and Bedzyk (1997) | Synthetic | MaSp1 | *P. pastoris* YFP5029 | 65–163 | 1000[c] |
| Arcidiacono et al. (1998) | cDNA | MaSp1 | *E. coli* BL21 (DE3) | 43 | 4 |
| Fukushima (1998) | Synthetic | MaSp1 | *E. coli* JM109 | 10–20 | 5 |
| Winkler et al. (2000) | Synthetic | MaSp1 | *E. coli* BLR (DE3) | 25 | 20 |
| Szela et al. (2000) | Synthetic | MaSp1 | *E. coli* BLR (DE3) | 25 | 10 |
| Xia et al. (2010) | Synthetic | MaSp1 | *E. coli* BL21 (DE3)[a] | 100–285 | 500–2700 |
| Lin et al. (2013) | Synthetic | TuSp1 + CTD | *E. coli* BL21 (DE3) | 189 | 40 |
| Xu et al. (2012) | Synthetic | AcSp1 | *E. coli* BL21 (DE3) | 19–76 | 22–80 |
| *Yeast* | | | | | |
| Fahnestock and Bedzyk (1997) | Synthetic | MaSp1 | *P. pastoris* YFP5029 | 65–163 | 1000[c] |
| *Mammalian cells* | | | | | |
| Lazaris et al. (2002) | cDNA | MaSp1 MaSp3 | Baby hamster kidney | 63–140 | 25–50 |
| *Plants* | | | | | |
| Scheller et al. (2001) | Synthetic | MaSp1 | Tobacco (*Nicotiana* sp.) Potato (*Solanum* sp.) | 100 | 0.1 g/5 g leaf |
| Hauptmann et al. (2013) | Synthetic | FLAG | Tobacco (*Nicotiana* sp.) | 47–250 | 1.8 mg/50 g leaf |

*Ibr* internal block repeat
[a]Genetically modified
[b]Purity >90 %
[c]Protein titer before purification

been reported for expression studies (Table 12.5). Unfortunately, the expression levels for the synthetic genes have been low, with the majority of the cases of the recombinant protein only representing 5 % of the total cellular protein. One of the most robust production levels have approached 1000 mg for 1 L of saturated *Pichia pastoris* cultures (Fahnestock and Bedzyk 1997). However, for most prokaryotic expression systems, the typical protein yields have been in the range of 10–50 mg/L after purification (>90 % purity) (Table 12.5).

Microorganisms have been the preferred choice as hosts for heterologous protein expression systems for spider silk proteins. Utilization of *E. coli* as a host system offers many benefits, including its fast replication time and low cost associated with culturing vast quantities of cells. Because *E. coli* has been heavily used by molecular biologists for cloning purposes, it also provides some of the best genetic tools available for regulating protein induction, methods for rapid purification of proteins, and techniques to circumvent recombinant proteins that display toxic effects when expressed in a prokaryotic background. Using *E. coli*, growth conditions can also be easily translated into an industrial scale format. The pharmaceutical industry has successfully used this system for large-scale protein production for numerous recombinant proteins for medicinal applications. Although chemists have developed strategies to form polymers from organic materials, it has been challenging to control the polymerization process using different building blocks, especially when attempting to design complex polymeric compounds with new biological functions. However, through the use of recombinant DNA approaches, scientists can more readily control the assembly of different DNA pieces to create protein polymers with programmed sequences, secondary structures, molecular weights and even enhance recombinant protein solubilities. In this process, scientists follow three basic steps: (i) design and assembly of synthetic silk-like segments, (ii) selection of a prokaryotic expression vector, followed by insertion and multimerization of synthetic silk-like DNA segments, and (iii) transformation, expression and purification of recombinant silk proteins from different bacterial clones. In some cases, the initial step (i) can be substituted by using different lengths of the natural spider silk cDNA sequences. Or, alternatively, a combination of synthetic silk-like genes can be coupled with pieces of the natural spider silk cDNAs.

### *12.4.3 Seamless Cloning Strategy to Produce Synthetic Spider Silk Genes*

We have employed a seamless cloning strategy with oligonucleotides that were codon-optimized for expression of *L. hesperus* MaSp1 block repeats in *E. coli* (Scior et al. 2011). Because the block repeat of MaSp1 is 25–35 amino acids, it would typically require the synthesis and annealing of two complementary oligonucleotides with lengths of approximately 120 nucleotides. However, because the upper limit on the synthesis of oligonucleotides is around 100 nucleotides, we

constructed the MaSp1 block repeat segment using two steps. First, two oligonucleotides were designed to span the 40 amino acids block repeat of MaSp1. For this design, we created two oligonucleotides that were perfectly complementary at their 3′ ends, but had singled-stranded 5′ ends that could be filled in by a heat-stable DNA polymerase after annealing to make double-stranded molecules (Fig. 12.5a). Once the synthetic block module for MaSp1 was generated, it was amplified with gene-specific primers and three different restriction sites were added to the ends of the internal block repeat (Fig. 12.5a). The forward primer was engineered to add the restriction sites *Sca*I, *Nde*I, and *Bsa*I. The incorporation of the *Sca*I site provided extra nucleotides on one end of the synthetic MaSp1 module to facilitate restriction digestion efficiency, while *Nde*I and *Bsa*I sites served to simplify insertion and seamless cloning in the prokaryotic expression vector pET-24a, respectively. The reverse primer was designed to add *Spe*I, *Sac*I, and *Bsm*BI restriction sites, with *Bsm*BI and *Sac*I being used for seamless cloning and *Sac*I also functioning to ligate the monomer MaSp1 internal block repeat into pET-24a. After insertion of the monomeric MaSp1 repeat (MaSp1 1X) into the *Nde*I and *Sac*I site of pET-24a to create pET-24a MaSp1 1X, this vector was used for expansion of the monomeric unit into dimeric (MaSp1 2X), tetrameric (MaSp1 4X), etc. repeats. For this to be accomplished the pET-24a MaSp1 1X vector was digested with *Bsa*I and *Sac*I to release the monomeric block repeat and ligated into the pET-24a MaSp1 1X plasmid after it was doubly digested with *Bsm*BI and *Sca*I (Fig. 12.5b). This allows for the multimerization of the MaSp1 1X block repeat without the creation of internal restriction sites during the doubling process, which would normally introduce two codons at the fusion junction specifying two amino acids (6-bp restriction site) that were not naturally found within the MaSp1 protein chain. Several rounds of cloning can be used to expand the repetitive block repeats to obtain sizes that approach the protein masses of native sized MaSp1 from spiders. After the conclusion of the block repeat expansion, amplification and insertion of natural cDNAs coding for the NTD and CTD can be readily inserted into the pET-24a vector *e.g.* pET-24a MaSp1 8X to form vectors that code for minifibroins or fibroins that approach the properties of native fibroins. This system also allows for the integration of adding 6 consecutive histidine residues (6x His tag) to the C-terminal region of the recombinant protein. The synthetic or hybrid silk genes inserted into the pET-24a vector are placed under the transcriptional control of the T7 promoter and require the addition of the inducer isopropyl-β-D-1-thiogalactopyranoside to initiate protein expression. However, it is worth noting that even with implementation of these creative strategies, there are still current barriers and challenges, largely due to the highly repetitive core sequences of the synthetic gene. This results in undesired homologous recombination of block repeats during replication in bacteria, transcriptional errors, unwanted translational pausing, and accumulation of vast quantities of recombinant proteins in inclusion bodies – all leading to lower yields of recombinant silk proteins.

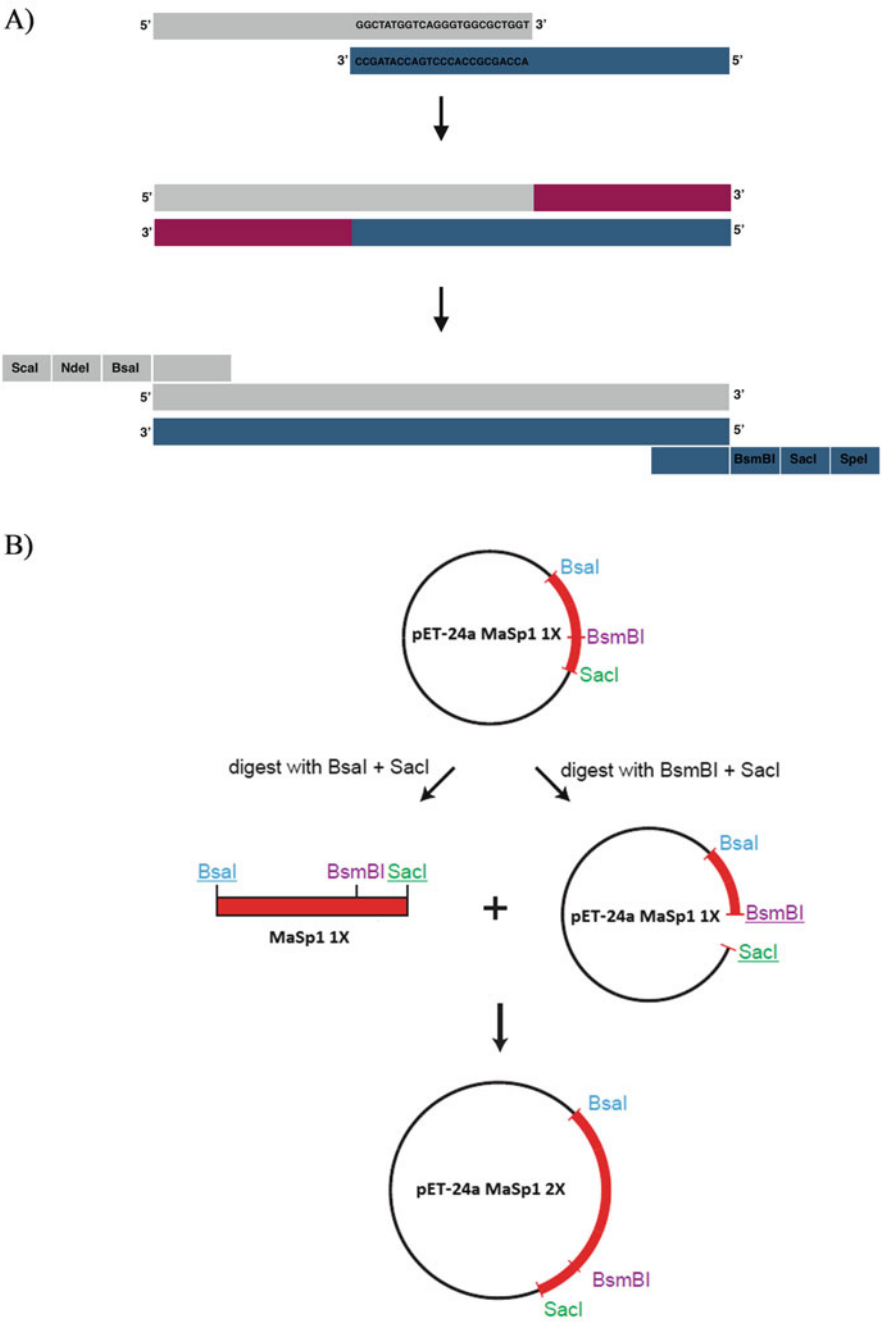


**Fig. 12.5** Molecular approach using oligonucleotides to build a single block repeat that can be multimerized by a seamless cloning strategy for expression studies. In this approach, the codons are optimized for the host organism used for expression. (**a**) Design of single block repeat; (**b**) Seamless cloning strategy used for expansion of single block repeat

### 12.4.4 Expression of Other Spidroin Family Members and Purification Methodologies

Although the main emphasis has involved optimization of MaSp-like recombinant protein expression in bacteria, reports involving synthesis of other spidroin family members, such as TuSp1, have been shown to be successful. In these studies, synthetic pieces of nucleic acids were codon-optimized and multimerized, to produce 11 copies of the internal block repeat units of *N. antipodiana* TuSp1 (Lin et al. 2013). In addition, the construct was designed to contain the CTD of MiSp1, forming a hybrid recombinant protein with a predicted molecular mass of 189-kDa. The rationale for fusing the MiSp1 CTD to the block repeats of TuSp1 (constructed named 11RPC), instead of using the MaSp1 or TuSp1 CTDs, resides in its differential solubility. The MiSp1 CTD shows much higher solubility in water, resulting in a lower propensity for premature aggregation during protein purification. To increase recombinant TuSp1 protein size, a serine residue within the MiSp1 CTD was mutated to a cysteine. This resulted in the 189-kDa monomeric unit that formed a 378-kDa dimeric unit through thiol oxidization by oxygen dissolved in solution. Although this construct is considerably larger than MaSp-based recombinant constructs, it also suffered from low expression levels, yielding only about 40 mg/L in shake flasks. Fibers spun from the purified recombinant proteins were shown to have higher breaking stress, but lower extensibility relative to natural tubuliform silk fibers (Lin et al. 2013).

Several different strategies have been explored to purify recombinant silk proteins from crude bacterial lysates. The vast majority of these approaches have focused on the utilization of N- or C-terminal His-tags, which allows for rapid purification of recombinant silk proteins in a single step by immobilized metal ion affinity chromatography (IMAC). However, affinity purification on a large-scale format is costly, time consuming, and a labor intensive endeavor. Currently, it is unclear whether the presence of the His-tag influences the secondary structure of the recombinant silk proteins and whether this additional sequence impacts spidroin assembly during the *in vitro* spinning process. Further studies will be required to determine whether the His-tag compromises the mechanical properties of synthetic fibers. Alternative strategies to purify recombinant silk proteins without the implementation of His-tags and metal ion affinity chromatography have been explored, including protocols that take advantage of the thermal stability and resistance of spider silk proteins to organic acids (Dams-Kozlowska et al. 2013).

Attempts to produce tougher spider silk fibers have led scientists to become quite industrious with their approaches. For example, researchers have created transgenic silkworms that encode chimeric silkworm/spider silk proteins. These transgenic silkworms can synthesize and secrete spider silk fibers into cocoons (Teule et al. 2012). These cocoons contain endogenous silk proteins from silkworms mixed with synthetic spider silk-like products resulting in composite fibers. These composites have mechanical properties that are, on average, tougher relative to parental silkworm silk fibers and as tough as natural dragline silk (Teule et al. 2012). Breaking

stress values for the composite fibers were about half of the tensile strength for natural dragline silk. In these studies, investigators manufactured synthetic composite fibers by expression of a fusion protein consisting of a 78-kDa synthetic spider silk protein linked to the enhanced green fluorescence protein (EGFP). Expression of the spider silk-EGFP fusion protein was targeted to the posterior silk gland by using a piggyBac vector containing the *B. mori* fibroin heavy chain promoter. Immunoblot analysis using lysate from the posterior silk gland region and an anti-GFP antibody for detection confirmed the expression of the fusion protein, which migrated at a molecular mass of approximately 116-kDa (Teule et al. 2012). Despite these promising results, one caveat of the study revealed that the mechanical properties of the composite silks from the transgenic animals displayed more variability relative to parental fibers. Moreover, different transgenic lines also produced composite silks that displayed varying tensile strengths, suggesting the lines express different silkworm/spider silk protein ratios and perhaps the localization of the proteins in the fibers is dissimilar. Whether the addition of GFP, which has a molecular mass of approximately 27 kDa, produced any adverse effects on the performance of the fibers is unclear, but the transgenic animals were capable of fiber formation with GFP attached to the synthetic spider silk protein. Other studies have generated transgenic silkworms that can express an 83-kDa MaSp1 recombinant protein lacking GFP; these transgenic silkworms were also capable of secreting MaSp1 into the fibers and the mechanical properties (breaking stress and strain) were shown to outperform the parental silkworm silk fibers (Wen et al. 2010).

## 12.5 Biomimicry of the Spinning Process, Applications and Products

### *12.5.1 Artificial Silk Fibers by Biomimicry*

Many studies have been exploring the production of artificial silk fibers. However, to date, no company or laboratory has reported a spinning process that produces synthetic fibers that mimic the mechanical properties of natural spider silk. In the scientific literature there have been a number of distinct protocols published that describe the formation of artificial silk fibers based upon the use of a spinning dope with purified recombinant silk proteins (Lazaris et al. 2002; Teule et al. 2009; Hsia et al. 2012). Most of these fibers have been produced using wet spinning through a coagulation bath, electrospinning, or approaches that incorporate microfluidic devices Rearrange. Many of these spinning methods have relied on the use of harsh organic solvents to dissolve the recombinant silk proteins, including lithium bromide (LiBr) and 1,1,1,3,3, 3-hexafluoro-2-propanol (HFIP) (Liivak et al. 1998; Min et al. 2004; Teule et al. 2009). Collectively, it is a challenging task to mimic the natural spinning process, which involves complex combinations of extrusion and drawing processes (Vollrath et al. 1998). The effective integration of these processes

distinguishes it from other methods of synthetic polymeric fiber production. Advances are being made through the use of microfluidic devices to understand the sequences of events and kinetics of silk assembly. However, the long-term goal is to integrate the knowledge obtained from the microfluidic device studies and transition it into the development of a large-scale biomimetic spinning process. Several independent labs are currently investigating this transition. In order to have success, there are many factors that will influence the drawing process, including the removal of water, the behavior of the spin-dope fluidity, and other environmental parameters e.g. temperature, humidity, and draw rate.

### *12.5.2 Spinning Dope*

While several steps are involved in the production of artificial spider silk, the first step requires preparation of the spinning dope, which is a liquid solution that contains the dissolved spidroins. Organic solvents are most commonly utilized to dissolve the purified recombinant spidroins that have been subject to lyophilization, providing strong hydrogen bonding properties to ensure effective solvent-protein interactions. Many organic solvents are efficient at solubilizing spidroins, but these solvents have many drawbacks or disadvantages. For example, the toxic effects associated with the molecules pose health concerns for biomedical applications. Despite this shortcoming, most scientists have turned to dissolving spidroin powder in HFIP, which allows spidroin concentrations in the range of 10–30 % (w/v), with the highest spidroin concentration being reported at 45–60 % (w/v) (Brooks et al. 2008; Hsia et al. 2012; Adrianos et al. 2013; Albertson et al. 2014). One advantage of using HFIP to dissolve the spidroins is its volatility, allowing investigators to dissolve the spidroin powder in larger volumes, followed by solvent evaporation and concentration of the dope for the spinning process. In addition, some labs have preferred to use formic acid as the solvent for the spinning dope (Peng et al. 2009). Although the use of organic solvents has allowed for the synthesis of artificial spider silk fibers, these solvents are too toxic for medical applications, carrying formidable health risks for patients. In addition, vast quantities of these solvents will undoubtedly result in higher production costs associated with organic waste disposal during large-scale synthesis. In order to circumvent the toxic effects of the organic solvents, several different approaches have been reported that focus on spinning artificial silk fibers from concentrated aqueous spidroin solutions. Strategies to produce highly concentrated spidroin solutions through aqueous buffer systems are being vigorously pursued by scientists, representing one of the most active research areas in the silk community (Stark et al. 2007; Grip et al. 2009; Heidebrecht et al. 2015). One approach has involved resuspending lyophilized recombinant spidroin pellets in 6 M guanidinium isothiocyanate (GdmSCN), followed by dialysis (molecular weight cut-off 6000–8000 Da) against buffers containing 50 mM Tris-HCl [pH = 8.0] and 100 mM NaCl (Heidebrecht et al. 2015). The addition of the NaCl functions to prevent unspecific protein aggregation. After

this step, the solution can be further dialyzed against a 20% (w/v) polyethylene glycol (PEG; 35-kDa) solution, serving to remove water from the recombinant protein solution, leading to spinning dope concentrations ranging from 10 to 17% (w/v) (Heidebrecht et al. 2015). One weaknesses of this methodology, however, is that spidroins are forced into a highly concentrated solution, hindering spidroin self-assemble into micellar-like particles that resemble *in vivo* complexes in spiders. Moreover, these spinning dopes appear to be less stable and more prone to aggregation relative to self-assembled spinning dopes. Self-assembled spinning dopes can be achieved by following the identical steps described above except of performing dialysis against PEG, the solution can be subject to dialysis against a phosphate-containing buffer (30–50 mM sodium phosphate pH = 7.2), which induces a liquid-liquid phase separation of the spidroin solution into a low density and high-density phase. The high-density micellar phase contains self-assembled spidroins; this approach yielded "biomimetic" spinning dope concentrations ranging between 9 and 11% (w/v) (Heidebrecht et al. 2015). Other strategies to produce high spidroin concentrations have included dialyzing elutions obtained from affinity chromatography against urea, sodium chloride, and sodium phosphate or Tris buffers, followed by high-speed centrifugation, and then concentration of spidroins by ultrafiltration (Arcidiacono et al. 2002). Lastly, other approaches have described methods to solvate traditionally insoluble recombinant spidroins using a quick, single step process, leading to nearly 100% solvation and recovery of these proteins without degradation (Jones et al. 2015). In all cases, scientists have been able to use these aqueous spidroin solutions to produce synthetic silk fibers.

### *12.5.3 Wet-Spinning and Post-spin Draw*

One common method to produce synthetic spider silk fibers is through a wet-spinning process, where spidroin dopes are extruded into dehydrating agents. A variety of different alcohols have been investigated to initiate fiber formation, including ethanol, methanol, and isopropanol. In some cases, water was added to the coagulation bath, slowing the coagulation rate of spidroins and serving as a plasticizing agent. This led to fibers that are less brittle. These processes have led to fibers that have diameter sizes in the micrometer range, with many of them ranging from 10 to 80 micrometers (Teule et al. 2009; Gnesa et al. 2012). This technique allows for slow fiber formation, which facilitates the alignment of spidroins during the extrusion step. During the wet-spinning protocol, the extrusion of the dope through the needle of the syringe is advantageous over other methods such as electrospinning, resulting in shear forces that mimic the natural extrusion pathway. This facilitates the alignment of spidroins into a structural hierarchy that is necessary to achieve outstanding material properties in fibers. Overall, this methodology, as outlined above, allows investigators to create spinning dopes formulated in organic or aqueous solvents and to spin fibers in a diverse range of coagulation baths that permits tunable mechanical properties. One weakness of wet-spinning protocols,

however, is that molecules from the organic solvent or coagulation bath can become trapped within synthetic silk fibers during polymer formation, requiring extensive soaking in water to remove contaminants. This can be an expensive and time-consuming process, especially if artificial fiber production is being carried out on a large-scale manufacturing format.

Spiders also intrinsically subjugate extruded fibers to post-spin draw, a process that leads to the production of threads with improved mechanical properties. Experiments have demonstrated that the rate of post-spin draw can have a profound impact on the quality of fibers (Carmichael et al. 1999; Albertson et al. 2014). $^{13}C$ NMR spectroscopy studies have shown that the fraction of alanine residues in β-sheet conformation increases as the reeling speed increases, which correlates to an enhancement of the mechanical properties (Liivak et al. 1997). Consistent with these observations, molecular modeling has shown that by tuning the size of the β-sheet nanocrystals, the strength and the toughness of the material can be modulated by reeling speed conditions (Nova et al. 2010). Moreover, depending upon the protein sequences and humidity conditions used for the spinning process, scientists may be able to control the supercontraction properties of the spun fibers. Thus, it will be important for material scientists to integrate post-spin draw procedures that are integrated into spinning processes in order to manufacture high-performance threads. Different solvents have been employed for spinning fibers and performing post-spin draw to explore their impact on fiber performance. Spinning spider dragline silk spun in an aqueous bath followed by post-spin draw resulted in stronger fibers (higher breaking stress, yield stress and Young's modulus), but these fibers have had lower extensibility (decrease in breaking strain) (Liu et al. 2005). The increased strength is attributed to the fact that spinning the fibers in water, as opposed to LiBr or HFIP, gives rise to increased molecular orientation of the protein chains, thus improving the mechanical properties. Thus, important aspects that mimic the natural spinning process will be designing artificial spinning ducts that resemble and function like normal ducts as well as engineering devices to recapitulate the influence of the post-spin draw.

### *12.5.4 Electrospinning and Microfluidic Devices*

Another technique that scientists have explored to produce artificial spider silk fibers has involved electrospinning, which creates fibers by exposing liquid droplets of recombinant spidroin spinning dopes to high voltage. In this process, polymer nanofibers are generated by the formation and elongation of an electrified fluid jet (Reneker and Yarin 2008). When the solution is exposed to high voltage, the body of the liquid becomes charged and electrostatic repulsion counteracts the surface tension, resulting in nanofibers that are deposited on a grounded collector as the droplets experience stretching during the procedure. This process does not rely on the chemistry of coagulation that is required by wet-spinning methodologies. For artificial spider silk fibers, electric fields of 4–30 kV with electrode distances of 2–25 cm have

been used for electrospinning protocols (Bini et al. 2006; Peng et al. 2009; Yu et al. 2013). In particular, this procedure can give rise to the formation of non-woven mats. Several different parameters are important for the formation of non-woven mats, including the viscosity of the dope, the concentration of the recombinant spidroins, the electrical conductivity and permeability of the solvent, and the nanofiber surface free energy (Greiner and Wendorff 2007). One advantage of electrospinning is that lower spidroin concentrations can be used to form fibers, but higher concentrations in the range of 10–30 % (w/v) are more effective for fiber formation (Zarkoob et al. 2004; Bini et al. 2006; Zhou et al. 2008). Low β-sheet content was reported from non-woven mats electrospun from spinning dopes dissolved in HFIP (Lang et al. 2013). Interaction of the electromagnetic field with spidroin molecules inhibits β-sheet formation, but stabilizes α-helical structures via hydrogen bond dipoles (Stephens et al. 2005). Although nanofibers can be deposited on a solid container, nanofibers can be collected in coagulation baths containing organic or aqueous-based solvents. When the nanofibers are collected employing coagulation baths (fiber diameter sizes of approximately 80–1000 nm), posttreatment of the electrospun fibers with alcohols or organic solvents is necessary to induce formation of water resistance and stable β-sheet structure (Lang et al. 2013). Exposure of nanofibers to alcohol vapors has proven more effective than immersing the fibers in alcohol baths because submersion of the nanofibers can alter fiber morphology, resulting in more flattened and partially fused threads at the intersection of multiple fibers (Bini et al. 2006; Lang et al. 2013). The mechanical properties of electrospun fibers have inferior properties relative to natural fibers; however, the non-woven meshes can be used for other products, including filter or biomedical applications, where natural silk mechanical properties are not a requirement (Bogush et al. 2009).

In addition to wet spinning and electrospinning, synthetic spider silk fibers have been produced by microfluidic devices using dilute recombinant spidroin mixtures (Rammensee et al. 2008). The use of microfluidic devices has been demonstrated to lead to artificial spider silk fibers, but higher flow rates were necessary to induce fiber assembly using low or medium concentrations of protein solutions (Rammensee et al. 2008). Fiber production using microfluidic devices have many advantages over the other two spinning methods, in that, such devices can be designed and engineered to mimic aspects of the natural extrusion process of spider silk. These aspects include being able to precisely control or adjust changes in pH, ion concentrations, and elongational flow conditions.

## *12.5.5 Applications and Products*

### 12.5.5.1 Fibers and Films

Although much attention has been placed on the development of artificial spider silk fibers for uses in ropes, cords, body armor and other engineering materials that are fiber-based, recombinant spider silk proteins can be processed into films, foams,

hydrogels, and nanoparticles for drug delivery. Recombinant spider silk protein films have potential for diverse applications, in particular for the medical community due to its biocompatibility (Allmeling et al. 2006). Biodegradable biomaterials that are implantable are attractive for devices that control the delivery of drugs in animals. Possible uses of films include materials for controlled release of substances at specific sites in the human body and cell supporting scaffolds (Sofia et al. 2001; Hardy et al. 2013). These films experience partial degradation in the presence of proteases associated with the wound healing process within 2 weeks, which is consistent with the timing of the normal tissue repair response (Muller-Hermann and Scheibel 2015). Micro-particles engineered to carry cargo, such as pharmaceutical drugs, could also be designed to allow for delayed drug release by coating particles with a layer of recombinant spider silk protein. Research has shown that recombinant spider silk protein films are chemically stable and transparent materials under ambient conditions (Huemmerich et al. 2006). The properties of the films are determined by the secondary structure of the protein chains, the intermolecular interactions of the chains, and the connections of the materials interface with the environment (Spiess et al. 2010). During the creation of films, recombinant spider silk proteins have been demonstrated to undergo structural transitions from either random coil or α-helical conformations to β-sheet-rich structures (Huemmerich et al. 2006). Treatment of the recombinant spider silk proteins with alcohol or kosmotropic salts was shown to lead to films that are β-sheet-rich, chemically stable and water insoluble. The stability of the films is directly linked to the β-sheet content, with increasing levels leading to films with higher strength and elastic modulus, but lower extensibility. The addition of the NTD or CTD on the recombinant spider silk construct, although important in the fiber spinning process, appear to have no substantial influence on the β-sheet formation, which is being controlled by the amino acid sequences of the internal block repeat modules. However, the presence of the NTD or CTDs have been shown to increase the chemical stability of the films (Slotta et al. 2006).

#### 12.5.5.2 Spider Silk Particles

Recombinant spider silk proteins are also suitable for construction of particles that can be utilized for a host of applications. These particles can be assembled and designed to carry low molecular weight molecules for drug delivery (Hardy et al. 2013). Diameter particle size can be adjustable by varying the recombinant protein concentration or mixing vigorously with the reagents used for salting out (Elsner et al. 2015). The intrinsic properties of spider silk proteins, which include slow biodegradability, poor immunogenicity, and low toxicity, make them highly suitable candidates to serve as particles that can carry a broad range of different organic molecules. Packaging of the drug can be facilitated by diffusion or co-precipitation of the recombinant spidroins. When loading the drug, it cannot display electrostatic repulsion with the recombinant spidroins. Therefore, depending upon the charge on the drug, spidroins can be designed with charges that are opposite of the drug to

facilitate packaging. Moreover, silk particles have been shown to retain their molecular properties in the human body for a period of time before degradation occurs (Muller-Hermann and Scheibel 2015). Experiments designed to investigate the uptake of the particles made of recombinant spider silk proteins have shown that mammalian cells uptake particles with a positive charge more efficiently than negatively-charged particles. Incorporation of cell penetrating peptides (*e.g.* RGD-functionalized spidroins) have been shown to increase the number of particles transported into HeLa cells (Elsner et al. 2015).

## 12.6 Summary and Future Challenges

Over the past three decades there has been substantial progress in understanding the protein sequences of the spidroin family members. This has been accelerated by scientific advances in gene cloning, DNA sequencing, transcriptomics, and proteomics. With each passing month, scientists are replacing partial cDNA sequences that code for spidroin family members with complete genomic DNA sequences. Currently, two major challenges exist in the spider silk community. The first involves development of methodologies that allow for expression of full-length recombinant spider silk proteins in high quantities, while the second challenge involves engineering a highly concentrated aqueous spinning dope that gives rise to high performance fibers. As more chemical details regarding the natural extrusion process of spider silk emerge, scientists are incorporating these concepts into the spinning process to mimic fiber synthesis. Many different spinning methods continue to be explored, including wet-spinning and electrospinning. Through the development of creative genetic engineering strategies, strides to manufacture recombinant proteins that approach native size spidroins are becoming more feasible, providing much excitement and promise for developing a wave of next generation biomaterials. Because spiders spin a host of different fiber types with distinct mechanical properties, scientists are eager to capitalize on the production of recombinant spider silk proteins for a wide range of diverse applications, including sutures for microsurgery, silk particles for drug delivery, scaffolds for tissue engineering, body armor, and construction of a vast array of novel engineering products. For example, as proof-of-concept the successful synthesis and purification of recombinant silk proteins resembling native size MaSp1 molecules via heterologous expression systems demonstrate that the first challenge can be solved. In addition, strategies to generate recombinant spidroin mixtures that resemble natural spinning dope properties are accelerating at a fast rate. Through the development of different chemical treatments, scientists are generating recombinant spidroins with secondary and tertiary structures that more accurately reflect the folded states of natural spidroins in spinning dopes. Thus, advances in expression of longer protein chain lengths, combined with improvements of recombinant spidroin processing to form more native-like spinning dopes, are putting the field in a position to spin higher performance fibers. Although the majority of research teams have focused on

expression of recombinant silk proteins and spinning of artificial fibers from dragline fiber components, little is known whether other members of the spidroin family may have other advantageous features, including improved expression, solubility, purification, and easier processing into final products. Additional studies will need to be performed to address these issues. In closing, it is an exciting moment in the history of spider silk biology and its uses of recombinant spider silk proteins.

**Acknowledgements** We thank Tiffany-Blasingame Tuton, Felicia Jeffery, Coby La Mattina, Albert Lin and Tyler Chuang for their contributions with the spider microdissection images from black widow spiders. In addition, we are grateful for contributions from Yang Hsia, Eric Gnesa, Thanh Pham, and Connie Liu.

## References

Adrianos SL, Teule F, Hinman MB, Jones JA, Weber WS, Yarger JL, Lewis RV (2013) *Nephila clavipes* flagelliform silk-like GGX motifs contribute to extensibility and spacer motifs contribute to strength in synthetic spider silk fibers. Biomacromolecules 14:1751–1760

Albertson AE, Teule F, Weber W, Yarger JL, Lewis RV (2014) Effects of different post-spin stretching conditions on the mechanical properties of synthetic spider silk fibers. J Mech Behav Biomed Mater 29:225–234

Allmeling C, Jokuszies A, Reimers K, Kall S, Vogt PM (2006) Use of spider silk fibres as an innovative material in a biocompatible artificial nerve conduit. J Cell Mol Med 10:770–777

Andersson M, Chen G, Otikovs M, Landreh M, Nordling K, Kronqvist N, Westermark P, Jornvall H, Knight S, Ridderstrale Y, Holm L, Meng Q, Jaudzems K, Chesler M, Johansson J, Rising A (2014) Carbonic anhydrase generates $CO_2$ and $H^+$ that drive spider silk formation via opposite effects on the terminal domains. PLoS Biol 12:e1001921

Arcidiacono S, Mello C, Kaplan D, Cheley S, Bayley H (1998) Purification and characterization of recombinant spider silk expressed in *Escherichia coli*. Appl Microbiol Biotechnol 49:31–38

Arcidiacono S, Mello CM, Butler M, Welsh E, Soares JW, Allen A, Ziegler D, Laue T, Chase S (2002) Aqueous processing and fiber spinning of recombinant spider silks. Macromolecules 35:1262–1266

Argintean S, Chen J, Kim M, Moore AMF (2006) Resilient silk captures prey in black widow cobwebs. Appl Phys A Mater Sci Process 82:235–241

Ayoub NA, Garb JE, Tinghitella RM, Collin MA, Hayashi CY (2007) Blueprint for a high-performance biomaterial: full-length spider dragline silk genes. PLoS One 2:e514

Ayoub NA, Garb JE, Kuelbs A, Hayashi CY (2013) Ancient properties of spider silks revealed by the complete gene sequence of the prey-wrapping silk protein (AcSp1). Mol Biol Evol 30:589–601

Bini E, Foo CW, Huang J, Karageorgiou V, Kitchel B, Kaplan DL (2006) RGD-functionalized bioengineered spider dragline silk biomaterial. Biomacromolecules 7:3139–3145

Blackledge TA, Summers AP, Hayashi CY (2005) Gumfooted lines in black widow cobwebs and the mechanical properties of spider capture silk. Zoology (Jena) 108:41–46

Blasingame E, Tuton-Blasingame T, Larkin L, Falick AM, Zhao L, Fong J, Vaidyanathan V, Visperas A, Geurts P, Hu X, La Mattina C, Vierra C (2009) Pyriform spidroin 1, a novel member of the silk gene family that anchors dragline silk fibers in attachment discs of the black widow spider, *Latrodectus hesperus*. J Biol Chem 284:29097–29108

Bogush VG, Sokolova OS, Davydova LI, Klinov DV, Sidoruk KV, Esipova NG, Neretina TV, Orchanskyi IA, Makeev VY, Tumanyan VG, Shaitan KV, Debabov VG, Kirpichnikov MP

(2009) A novel model system for design of biomaterials based on recombinant analogs of spider silk proteins. J Neuroimmune Pharmacol 4:17–27
Bon M (1710) A discourse upon the usefulness of the silk of spiders. Philos Trans 27:2–16
Brooks AE, Stricker SM, Joshi SB, Kamerzell TJ, Middaugh CR, Lewis RV (2008) Properties of synthetic spider silk fibers based on *Argiope aurantia* MaSp2. Biomacromolecules 9:1506–1510
Carmichael S, Barghout JY, Viney C (1999) The effect of post-spin drawing on spider silk microstructure: a birefringence model. Int J Biol Macromol 24:219–226
Casem ML, Turner D, Houchin K (1999) Protein and amino acid composition of silks from the cob weaver, *Latrodectus hesperus* (black widow). Int J Biol Macromol 24:103–108
Chaw RC, Correa-Garhwal SM, Clarke TH, Ayoub NA, Hayashi CY (2015) Proteomic evidence for components of spider silk synthesis from black widow silk glands and fibers. J Proteome Res 14:4223–4231
Chen G, Liu X, Zhang Y, Lin S, Yang Z, Johansson J, Rising A, Meng Q (2012) Full-length minor ampullate spidroin gene sequence. PLoS One 7:e52293
Choresh O, Bayarmagnai B, Lewis RV (2009) Spider web glue: two proteins expressed from opposite strands of the same DNA sequence. Biomacromolecules 10:2852–2856
Clarke TH, Garb JE, Hayashi CY, Haney RA, Lancaster AK, Corbett S, Ayoub NA (2014) Multi-tissue transcriptomics of the black widow spider reveals expansions, co-options, and functional processes of the silk gland gene toolkit. BMC Genomics 15:365
Colgin MA, Lewis RV (1998) Spider minor ampullate silk proteins contain new repetitive sequences and highly conserved non-silk-like "spacer regions". Protein Sci 7:667–672
Dams-Kozlowska H, Majer A, Tomasiewicz P, Lozinska J, Kaplan DL, Mackiewicz A (2013) Purification and cytotoxicity of tag-free bioengineered spider silk proteins. J Biomed Mater Res A 101:456–464
Dicko C, Knight D, Kenney JM, Vollrath F (2004a) Secondary structures and conformational changes in flagelliform, cylindrical, major, and minor ampullate silk proteins. Temperature and concentration effects. Biomacromolecules 5:2105–2115
Dicko C, Vollrath F, Kenney JM (2004b) Spider silk protein refolding is controlled by changing pH. Biomacromolecules 5:704–710
Eberhard WG (2010) Possible functional significance of spigot placement on the spinnerets of spiders. J Arachnol 38:407–414
Elsner MB, Herold HM, Muller-Herrmann S, Bargel H, Scheibel T (2015) Enhanced cellular uptake of engineered spider silk particles. Biomater Sci 3:543–551
Fahnestock SR, Bedzyk LA (1997) Production of synthetic spider dragline silk protein in *Pichia pastoris*. Appl Microbiol Biotechnol 47:33–39
Fahnestock SR, Irwin SL (1997) Synthetic spider dragline silk proteins and their production in *Escherichia coli*. Appl Microbiol Biotechnol 47:23–32
Fukushima Y (1998) Genetically engineered syntheses of tandem repetitive polypeptides consisting of glycine-rich sequence of spider dragline silk. Biopolymers 45:269–279
Gaines WA, Sehorn MG, Marcotte WR (2010) Spidroin N-terminal domain promotes a pH-dependent association of silk proteins during self-assembly. J Biol Chem 285:40745–40753
Garb JE, Hayashi CY (2005) Modular evolution of egg case silk genes across orb-weaving spider superfamilies. Proc Natl Acad Sci U S A 102:11379–11384
Gatesey J, Hayashi C, Motriuk D, Woods J, Lewis R (2001) Extreme diversity, conservation, and convergence of spider silk fibroin sequences. Science 291:2603–2605
Gerritsen VB (2002) The tiptoe of an airbus. Protein Spotlight Swiss Prot 24:1–2
Geurts P, Zhao L, Hsia Y, Gnesa E, Tang S, Jeffery F, La Mattina C, Franz A, Larkin L, Vierra C (2010a) Synthetic spider silk fibers spun from Pyriform Spidroin 2, a glue silk protein discovered in orb-weaving spider attachment discs. Biomacromolecules 11:3495–3503
Geurts P, Zhao L, Hsia Y, Gnesa E, Tang S, Jeffery F, Mattina CL, Franz A, Larkin L, Vierra C (2010b) Synthetic spider silk fibers spun from pyriform spidroin 2, a glue silk protein discovered in orb-weaving spider attachment discs. Biomacromolecules 11:3495–3503

Gnesa E, Hsia Y, Yarger JL, Weber W, Lin-Cereghino J, Lin-Cereghino G, Tang S, Agari K, Vierra C (2012) Conserved C-terminal domain of spider tubuliform spidroin 1 contributes to extensibility in synthetic fibers. Biomacromolecules 13:304–312

Gosline JM, Guerrete PA, Ortlepp CS, Savage KN (1999) The mechanical design of spider silks: from fibroin sequence to mechanical function. J Exp Biol 202:3295–3303

Greiner A, Wendorff JH (2007) Electrospinning: a fascinating method for the preparation of ultrathin fibers. Angew Chem Int Ed 46:5670–5703

Grip S, Johansson J, Hedhammar M (2009) Engineered disulfides improve mechanical properties of recombinant spider silk. Protein Sci 18:1012–1022

Guerette PA, Ginzinger DG, Weber BH, Gosline JM (1996) Silk properties determined by gland-specific expression of a spider fibroin gene family. Science 272:112–115

Guinea GV, Elices M, Plaza GR, Perea GB, Daza R, Riekel C, Agullo-Rueda F, Hayashi C, Zhao Y, Perez-Rigueiro J (2012) Minor ampullate silks from *Nephila* and *Argiope* spiders: tensile properties and microstructural characterization. Biomacromolecules 13:2087–2098

Hagn F, Eisoldt L, Hardy JG, Vendrely C, Coles M, Scheibel T, Kessler H (2010) A conserved spider silk domain acts as a molecular switch that controls fibre assembly. Nature 465:239–242

Hardy JG, Leal-Egana A, Scheibel TR (2013) Engineered spider silk protein-based composites for drug delivery. Macromol Biosci 13:1431–1437

Hauptmann V, Weichert N, Menzel M, Knoch D, Paege N, Scheller J, Spohn U, Conrad U, Gils M (2013) Native-sized spider silk proteins synthesized in planta via intein-based multimerization. Transgenic Res 22:369–377

Hayashi C, Lewis RV (1998) Evidence from flagelliform silk cDNA for the structural basis of elasticity and modular nature of spider silks. J Mol Biol 275:773–784

Hayashi CY, Lewis RV (2000) Molecular architecture and evolution of a modular spider silk protein gene. Science 287:1477–1479

Hayashi CY, Shipley NH, Lewis RV (1999) Hypotheses that correlate the sequence, structure, and mechanical properties of spider silk proteins. Int J Biol Macromol 24:271–275

Hayashi CY, Blackledge TA, Lewis RV (2004) Molecular and mechanical characterization of aciniform silk: uniformity of iterated sequence modules in a novel member of the spider silk fibroin gene family. Mol Biol Evol 21:1950–1959

Heidebrecht A, Eisoldt L, Diehl J, Schmidt A, Geffers M, Lang G, Scheibel T (2015) Biomimetic fibers made of recombinant spidroins with the same toughness as natural spider silk. Adv Mater 27:2189–2194

Hinman MB, Lewis RV (1992) Isolation of a clone encoding a second dragline silk fibroin. *Nephila clavipes* dragline silk is a two-protein fiber. J Biol Chem 267:19320–19324

Hsia Y, Gnesa E, Pacheco R, Kohler K, Jeffery F, Vierra C (2012) Synthetic spider silk production on a laboratory scale. J Vis Exp 2012:e4191

Hu X, Kohler K, Falick AM, Moore AM, Jones PR, Sparkman OD, Vierra C (2005a) Egg case protein-1. A new class of silk proteins with fibroin-like properties from the spider *Latrodectus hesperus*. J Biol Chem 280:21220–21230

Hu X, Lawrence B, Kohler K, Falick AM, Moore AM, Mcmullen E, Jones PR, Vierra C (2005b) Araneoid egg case silk: a fibroin with novel ensemble repeat units from the black widow spider, *Latrodectus hesperus*. Biochemistry 44:10020–10027

Hu X, Kohler K, Falick AM, Moore AM, Jones PR, Vierra C (2006a) Spider egg case core fibers: trimeric complexes assembled from TuSp1, ECP-1, and ECP-2. Biochemistry 45:3506–3516

Hu X, Vasanthavada K, Kohler K, Mcnary S, Moore AM, Vierra CA (2006b) Molecular mechanisms of spider silk. Cell Mol Life Sci 63:1986–1999

Hu X, Yuan J, Wang X, Vasanthavada K, Falick AM, Jones PR, La Mattina C, Vierra CA (2007) Analysis of aqueous glue coating proteins on the silk fibers of the cob weaver, *Latrodectus hesperus*. Biochemistry 46:3294–3303

Huemmerich D, Slotta U, Scheibel T (2006) Processing and modification of films made from recombinant spider silk proteins. Appl Phys A 82:219–222

Ittah S, Michaeli A, Goldblum A, Gat U (2007) A model for the structure of the C-terminal domain of dragline spider silk and the role of its conserved cysteine. Biomacromolecules 8:2768–2773

Jain D, Zhang C, Cool LR, Blackledge TA, Wesdemiotis C, Miyoshi T, Dhinojwala A (2015) Composition and function of spider glues maintained during the evolution of cobwebs. Biomacromolecules 16:3373–3380

Jeffery F, La Mattina C, Tuton-Blasingame T, Hsia Y, Gnesa E, Zhao L, Franz A, Vierra C (2011) Microdissection of black widow spider silk-producing glands. J Vis Exp 47:2382. doi:10.3791/2382

Jin HJ, Kaplan DL (2003) Mechanism of silk processing in insects and spiders. Nature 424:1057–1061

Jones JA, Harris TI, Tucker CL, Berg KR, Christy SY, Day BA, Gaztambide DA, Needham NJ, Ruben AL, Oliveira PF, Decker RE, Lewis RV (2015) More than just fibers: an aqueous method for the production of innovative recombinant spider silk protein materials. Biomacromolecules 16:1418–1425

Knight DP, Vollrath F (2001) Changes in element composition along the spinning duct in a *Nephila* spider. Naturwissenschaften 88:179–182

Kohler K, Thayer W, Le T, Sembhi A, Vasanthavada K, Moore AM, Vierra C (2005) Characterization of a novel class II bHLH transcription factor from the black widow spider, *Latrodectus hesperus*, with silk-gland restricted patterns of expression. DNA Cell Biol 24:371–380

Kovoor J, Zylberberg L (1980) Fine structural aspects of silk secretion in a spider (*Araneus diadematus*). I. Elaboration in the pyriform glands. Tissue Cell 12:547–556

Kovoor J, Zylberberg L (1982) Fine structural aspects of silk secretion in a spider. II. Conduction in the pyriform glands. Tissue Cell 14:519–530

Kummerlen J, Van Beek JD, Vollrath F, Meier B (1996) Local structure in spider dragline silk investigated by two-dimensional spin-diffusion nuclear magnetic resonance. Macromolecules 29:2920–2928

La Mattina C, Reza R, Hu X, Falick AM, Vasanthavada K, Mcnary S, Yee R, Vierra C (2008) Spider minor ampullate silk proteins are constituents of prey wrapping silk in the cob weaver *Latrodectus hesperus*. Biochemistry 47:4692–4700

Lane AK, Hayashi CY, Whitworth GB, Ayoub NA (2013) Complex gene expression in the dragline silk producing glands of the Western black widow (*Latrodectus hesperus*). BMC Genomics 14:846

Lang G, Jokisch S, Scheibel T (2013) Air filter devices including nonwoven meshes of electrospun recombinant spider silk proteins. J Vis Exp 2013:e50492

Lazaris A, Arcidiacono S, Huang Y, Zhou JF, Duguay F, Chretien N, Welsh EA, Soares JW, Karatzas CN (2002) Spider silk fibers spun from soluble recombinant silk produced in mammalian cells. Science 295:472–476

Lefevre T, Rousseau ME, Pezolet M (2007) Protein secondary structure and orientation in silk as revealed by Raman spectromicroscopy. Biophys J 92:2885–2895

Lefevre T, Boudreault S, Cloutier C, Pezolet M (2011) Diversity of molecular transformations involved in the formation of spider silks. J Mol Biol 405:238–253

Lewis R (1996) Unraveling the weave of spider silk. Bioscience 46:636–638

Lewis RV, Hinman M, Kothakota S, Fournier MJ (1996) Expression and purification of a spider silk protein: a new strategy for producing repetitive proteins. Protein Expr Purif 7:400–406

Liivak O, Flores A, Lewis L, Jelinski LW (1997) Conformation of the polyalanine repeats in minor ampullate gland silk of the spider *Nephila clavipes*. Macromolecules 30:7127–7130

Liivak O, Blye A, Shah N, Jelinski LW (1998) A microfabricated wet-spinning apparatus to spin fibers of silk proteins. Structure-property correlations. Macromolecule 31:2927–2951

Lin Z, Deng Q, Liu XY, Yang D (2013) Engineered large spider eggcase silk protein for strong artificial fibers. Adv Mater 25:1216–1220

Liu Y, Shao Z, Vollrath F (2005) Extended wet-spinning can modify spider silk properties. Chem Commun 19:2489–2491

Min BM, Lee G, Kim SH, Nam YS, Lee TS, Park WH (2004) Electrospinning of silk fibroin nanofibers and its effect on the adhesion and spreading of normal human keratinocytes and fibroblasts *in vitro*. Biomaterials 25:1289–1297

Muller-Hermann S, Scheibel T (2015) Enzymatic degradation of films, particles, and nonwoven meshes made of a recombinant spider silk protein. ACS Biomater Sci Eng 1:247–259

Nova A, Keten S, Pugno NM, Redaelli A, Buehler MJ (2010) Molecular and nanostructural mechanisms of deformation, strength and toughness of spider silk fibrils. Nano Lett 10:2626–2634

Parnham S, Gaines WA, Duggan BM, Marcotte WR, Hennig M (2011) NMR assignments of the N-terminal domain of *Nephila clavipes* spidroin 1. Biomol NMR Assign 5:131–133

Peng H, Zhou S, Jiang J, Guo T, Zheng X, Yu X (2009) Pressure-induced crystal memory effect of spider silk proteins. J Phys Chem B 113:4636–4641

Perry DJ, Bittencourt D, Siltberg-Liberles J, Rech EL, Lewis RV (2010) Piriform spider silk sequences reveal unique repetitive elements. Biomacromolecules 11:3000–3006

Pham T, Chuang T, Lin A, Joo H, Tsai J, Crawford T, Zhao L, Hsia Y, Williams C, Vierra CA (2014) Dragline silk: a fiber assembled with low-molecular-weight cysteine-rich proteins. Biomacromolecules 15:4073–4081

Prince JT, Mcgrath KP, Digirolamo CM, Kaplan DL (1995) Construction, cloning, and expression of synthetic genes encoding spider dragline silk. Biochemistry 34:10879–10885

Rabotyagova OS, Cebe P, Kaplan DL (2009) Self-assembly of genetically engineered spider silk block copolymers. Biomacromolecules 10:229–236

Rammensee S, Slotta U, Scheibel T, Bausch AR (2008) Assembly mechanism of recombinant spider silk proteins. Proc Natl Acad Sci U S A 105:6590–6595

Reneker DH, Yarin AL (2008) Electrospinning jets and polymer nanofibers. Polymer 49:2387–2425

Scheller J, Guhrs KH, Grosse F, Conrad U (2001) Production of spider silk proteins in tobacco and potato. Nat Biotechnol 19:573–577

Scior A, Preissler S, Koch M, Deuerling E (2011) Directed PCR-free engineering of highly repetitive DNA sequences. BMC Biotechnol 11:87

Slotta U, Tammer M, Kremer F, Koelsch P, Scheibel T (2006) Structural analysis of spider silk films. Supramol Chem 18:465–471

Sofia S, Mccarthy MB, Gronowicz G, Kaplan DL (2001) Functionalized silk-based biomaterials for bone formation. J Biomed Mater Res 54:139–148

Spiess L, Wohlrab S, Scheibel T (2010) Structural characterization and functionalization of engineered spider silk films. Soft Matter 6:4168–4174

Stark M, Grip S, Rising A, Hedhammar M, Engstrom W, Hjalm G, Johansson J (2007) Macroscopic fibers self-assembled from recombinant miniature spider silk proteins. Biomacromolecules 8:1695–1701

Stephens JS, Fahnestock SR, Farmer RS, Kiick KL, Chase DB, Rabolt JF (2005) Effects of electrospinning and solution casting protocols on the secondary structure of a genetically engineered dragline spider silk analogue investigated via Fourier transform Raman spectroscopy. Biomacromolecules 6:1405–1413

Szela S, Avtges P, Valluzzi R, Winkler S, Wilson D, Kirschner D, Kaplan DL (2000) Reduction-oxidation control of beta-sheet assembly in genetically engineered silk. Biomacromolecules 1:534–542

Teule F, Cooper AR, Furin WA, Bittencourt D, Rech EL, Brooks A, Lewis RV (2009) A protocol for the production of recombinant spider silk-like proteins for artificial fiber spinning. Nat Protoc 4:341–355

Teule F, Miao YG, Sohn BH, Kim YS, Hull JJ, Fraser MJ Jr, Lewis RV, Jarvis DL (2012) Silkworms transformed with chimeric silkworm/spider silk genes spin composite silk fibers with improved mechanical properties. Proc Natl Acad Sci U S A 109:923–928

Tian M, Lewis RV (2005) Molecular characterization and evolutionary study of spider tubuliform (eggcase) silk protein. Biochemistry 44:8006–8012

Tian M, Lewis RV (2006) Tubuliform silk protein: a protein with unique molecular characteristics and mechanical properties in the spider silk fibroin family. Appl Phys A 82:265–273
Tillinghast EK, Townley MA, Bernstein DT, Gallagher KS (1991) Comparative study of orb web hygroscopicity and adhesive spiral composition in three araneid spiders. J Exp Zool 259:154–165
Townley MA, Pu Q, Zercher CK, Neefus CD, Tillinghast EK (2012) Small organic solutes in sticky droplets from orb webs of the spider Zygiella atrica (Araneae; Araneidae): beta-alaninamide is a novel and abundant component. Chem Biodivers 9:2159–2174
Tremblay ML, Xu L, Lefevre T, Sarker M, Orrell KE, Leclerc J, Meng Q, Pezolet M, Auger M, Liu XQ, Rainey JK (2015) Spider wrapping silk fibre architecture arising from its modular soluble protein precursor. Sci Rep 5:11502
Van Beek JD, Hess S, Vollrath F, Meier BH (2002) The molecular structure of spider dragline silk: folding and orientation of the protein backbone. Proc Natl Acad Sci U S A 99:10266–10271
Vasanthavada K, Hu X, Falick AM, La Mattina C, Moore AM, Jones PR, Yee R, Reza R, Tuton T, Vierra C (2007) Aciniform spidroin, a constituent of egg case sacs and wrapping silk fibers from the black widow spider *Latrodectus hesperus*. J Biol Chem 282:35088–35097
Vasanthavada K, Hu X, Tuton-Blasingame T, Hsia Y, Sampath S, Pacheco R, Freeark J, Falick AM, Tang S, Fong J, Kohler K, La Mattina-Hawkins C, Vierra C (2012) Spider glue proteins have distinct architectures compared with traditional spidroin family members. J Biol Chem 287:35986–35999
Vollrath F, Edmonds DT (1989) Modulation of the mechanical properties of spider silk by coating with water. Nature 340:305–307
Vollrath F, Knight DP (1999) Structure and function of the silk production pathway in the spider *Nephila edulis*. Int J Biol Macromol 24:243–249
Vollrath F, Knight DP (2001) Liquid crystalline spinning of spider silk. Nature 410:541–548
Vollrath F, Fairbrother WJ, Williams RJP, Tillinghast EK, Bernstein DT, Gallagher KS, Townley MA (1990) Compounds in the droplets of the orb spider's viscid spiral. Nature 345:526–528
Vollrath F, Wen Hu X, Knight DP (1998) Silk production in a spider involves acid bath treatment. Proc R Soc B 263:817–820
Wen H, Lan X, Zhang Y, Zhao T, Wang Y, Kajiura Z, Nakagaki M (2010) Transgenic silkworms (*Bombyx mori*) produce recombinant spider dragline silk in cocoons. Mol Biol Rep 37:1815–1821
Winkler S, Szela S, Avtges P, Valluzzi R, Kirschner DA, Kaplan D (1999) Designing recombinant spider silk proteins to control assembly. Int J Biol Macromol 24:265–270
Winkler S, Wilson D, Kaplan DL (2000) Controlling beta-sheet assembly in genetically engineered silk by enzymatic phosphorylation/dephosphorylation. Biochemistry 39:12739–12746
Wolff JO, Grawe I, Wirth M, Karstedt A, Gorb SN (2015) Spider's super-glue: thread anchors are composite adhesives with synergistic hierarchical organization. Soft Matter 11:2394–2403
Xia XX, Qian ZG, Ki CS, Park YH, Kaplan DL, Lee SY (2010) Native-sized recombinant spider silk protein produced in metabolically engineered *Escherichia coli* results in a strong fiber. Proc Natl Acad Sci U S A 107:14059–14063
Xu M, Lewis RV (1990) Structure of a protein superfiber: spider dragline silk. Proc Natl Acad Sci U S A 87:7120–7124
Xu L, Rainey JK, Meng Q, Liu XQ (2012) Recombinant minimalist spider wrapping silk proteins capable of native-like fiber formation. PLoS One 7:e50227
Xu L, Tremblay ML, Orrell KE, Leclerc J, Meng Q, Liu XQ, Rainey JK (2013) Nanoparticle self-assembly by a highly stable recombinant spider wrapping silk protein subunit. FEBS Lett 587:3273–3280
Yu Q, Xu S, Zhang H, Gu L, Xu Y, Ko F (2013) Structure-property relationship of regenerated spider silk protein nano/microfibrous scaffold fabricated by electrospinning. J Biomed Mater Res A 102:3828–3837
Zarkoob S, Eby RK, Reneker DH, Hudson SD, Ertley D, Adams WW (2004) Structure and morphology of electrospun silk nanofibers. Polymer 45:3973–3977

Zhao AC, Zhao TF, Nakagaki K, Zhang YS, Sima YH, Miao YG, Shiomi K, Kajiura Z, Nagata Y, Takadera M, Nakagaki M (2006) Novel molecular and mechanical properties of egg case silk from wasp spider, *Argiope bruennichi*. Biochemistry 45:3348–3356

Zhao Y, Ayoub NA, Hayashi CY (2010) Chromosome mapping of dragline silk genes in the genomes of widow spiders (Araneae, Theridiidae). PLoS One 5:e12804

Zhou S, Peng H, Yu X, Zheng X, Cui W, Zhang Z, Li X, Wang J, Weng J, Jia W, Li F (2008) Preparation and characterization of a novel electrospun spider silk fibroin/poly(D, L-lactide) composite fiber. J Phys Chem B 112:11209–11216